Short Report

CHD7 mutations in patients initially diagnosed with Kallmann syndrome – the clinical overlap with CHARGE syndrome

Jongmans MCJ, van Ravenswaaij-Arts CMA, Pitteloud N, Ogata T, Sato N, Claahsen-van der Grinten HL, van der Donk K, Seminara S, Bergman JEH, Brunner HG, Crowley Jr WF, Hoefsloot LH. *CHD7* mutations in patients initially diagnosed with Kallmann syndrome – the clinical overlap with CHARGE syndrome.
Clin Genet 2009: 75: 65–71. © Blackwell Munksgaard, 2008

Kallmann syndrome (KS) is the combination of hypogonadotropic hypogonadism and anosmia or hyposmia, two features that are also frequently present in CHARGE syndrome. CHARGE syndrome is caused by mutations in the *CHD7* gene. We performed analysis of *CHD7* in 36 patients with KS and 20 patients with normosmic idiopathic hypogonadotropic hypogonadism (nIHH) in whom mutations in *KAL1*, *FGFR1*, *PROK2* and *PROKR2* genes were excluded. Three of 56 KS/ nIHH patients had *de novo* mutations in *CHD7*. In retrospect, these three *CHD7*-positive patients showed additional features that are seen in CHARGE syndrome. *CHD7* mutations can be present in KS patients who have additional features that are part of the CHARGE syndrome phenotype. We did not find mutations in patients with isolated KS. These findings imply that patients diagnosed with hypogonadotropic hypogonadism and anosmia should be screened for clinical features consistent with CHARGE syndrome. If such features are present, particularly deafness, dysmorphic ears and/or hypoplasia or aplasia of the semicircular canals, *CHD7* sequencing is recommended.

MCJ Jongmans[a], CMA van Ravenswaaij-Arts[b], N Pitteloud[c], T Ogata[d], N Sato[d], HL Claahsen-van der Grinten[e], K van der Donk[a], S Seminara[c], JEH Bergman[b], HG Brunner[a], WF Crowley Jr[c] and LH Hoefsloot[a]

[a]Department of Human Genetics, Radboud University Nijmegen Medical Center, Nijmegen, The Netherlands, [b]Department of Genetics, University Medical Center Groningen, Groningen University, The Netherlands, [c]Harvard Reproductive Endocrine Sciences Center and The Reproductive Endocrine Unit, Department of Medicine, Massachusetts General Hospital, Boston, MA, USA, [d]Department of Endocrinology and Metabolism, National Research Institute for Child Health and Development, Tokyo, Japan, and [e]Department of Pediatric Endocrinology, Radboud University Nijmegen Medical Center, Nijmegen, The Netherlands

Kallmann syndrome (KS) is a congenital disorder that combines hypogonadotropic hypogonadism and anosmia (1). Three modes of inheritance have been described: X-linked recessive, autosomal dominant and more rarely autosomal recessive.

To date, several genes have been identified to cause KS, either alone or in combination. Mutations in these genes together account for approximately 30% of all cases. *KAL1* encodes the protein anosmin and is involved in the X-linked

form of KS (KAL1, OMIM #308700) (2, 3). Loss-of-function mutations in the fibroblast growth factor receptor-1 gene (*FGFR1*) cause a form of KS (KAL2, OMIM #147950) that is generally inherited in an autosomal dominant way (4, 5). Dodé et al. reported in a further 10% of patients mutations in the prokineticin receptor-2 (*PROKR2*, KAL3, OMIM #607123) and prokineticin-2 (*PROK2*, KAL4, OMIM #607002) genes, encoding a cell surface receptor and one of its ligands, respectively (6). Mutations of the ligand, *PROK2*, can cause KS as well as normosmic idiopathic hypogonadotropic hypogonadism (nIHH) within the same family (6, 7). The same intrafamilial phenotypic variability is seen in patients with *FGFR1* mutations (4). Thus, KS is a phenotypically and genotypically heterogeneous disorder. Not only the degree of hypogonadism and anosmia may vary significantly but also other symptoms including bimanual synkinesia and dental agenesis (*KAL1* and *FGFR1*), renal anomalies (*KAL1*) and cleft lip/palate (*FGFR1*) occur with variable frequency (8).

CHARGE syndrome (OMIM #214800) is an autosomal dominant condition characterized by a variety of congenital anomalies including coloboma, heart defects, choanal atresia, retarded growth and development, genital hypoplasia, ear anomalies and deafness. Other commonly observed congenital defects are semicircular canal hypoplasia, facial nerve palsy, cleft lip/palate and tracheo-esophageal fistula (9). Our group has discovered *CHD7* as the causative gene in CHARGE syndrome (10). Since this discovery, several authors have reported on the phenotypic spectrum of *CHD7*-positive patients, including patients without typical CHARGE syndrome (11–13). Therefore, we presume that the mild end of the phenotypic spectrum of *CHD7* mutations is not yet completely explored.

Recent studies revealed that anosmia and abnormal olfactory bulb development, as well as hypogonadotropic hypogonadism, are almost consistent findings in CHARGE syndrome, indicating that the key features of KS are also present in CHARGE syndrome (14–16). For this reason, it has been suggested by others that *CHD7* may be considered a candidate locus in suspected KS cases without known mutations (8). This hypothesis is worthwhile exploring, also because mutations in *CHD7* can result in a much milder phenotype than the classical CHARGE syndrome phenotype. Therefore, we sequenced *CHD7* in a large group of patients diagnosed as KS or nIHH but without mutations in *KAL1*, *FGFR1*, *PROK2* and *PROKR2*.

Materials and methods

Patients

A cohort of seven Japanese patients with a clinical diagnosis of KS, without mutations in *KAL1*, *FGFR1*, *PROK2* and *PROKR2*, was screened for *CHD7* mutations (17). The diagnosis KS in this cohort was based on an underdevelopment of secondary sexual characteristics in combination with anosmia or hyposmia. Subsequently, the cohort was enlarged by 49 *KAL1*, *FGFR1*, *PROK2* and *PROKR2* negative North American patients with KS or nIHH. GnRH deficiency in this cohort was defined by (a) absent/incomplete puberty by age 18 year; (b) serum testosterone <100 ng/dl in men or estradiol <20 pg/ml in women in association with low or normal levels of serum gonadotropins; (c) otherwise normal pituitary function; (d) normal serum ferritin concentrations; and (e) normal magnetic resonance imaging (MRI) of the hypothalamic-pituitary region (5).

The patients in whom *CHD7* mutations were identified were carefully evaluated for clinical features of CHARGE syndrome. The *CHD7* gene was analyzed in the parents. The patients or their legal representatives gave informed consent for the DNA studies and the collection of clinical data. The studies were approved by the institutional review boards.

Mutation screening

DNA was isolated according to standard procedures. The 37 coding exons of the *CHD7* gene (exon 2–38, accession number NM_017780, NCBI) and their flanking intron sequences were amplified by polymerase chain reaction (PCR). Subsequently, sequence analysis was performed using a 3730 automated sequencer (Applied Biosystems, Foster City, CA). Primer information and PCR conditions are given in a previous report of our group (11).

The DNA samples of 11 mutation-negative patients were subsequently screened for exon deletions and/or duplications of the *CHD7* gene by multiplex ligation probe dependent amplification (MLPA) analysis (Table 1). We used a commercially available set of probes, the SALSA P201 kit (MRC-Holland, Amsterdam, The Netherlands; http://www.mrc-holland.com). Further details are described in our recent report on MLPA analysis of the *CHD7* gene (18).

Results

The *CHD7* gene was first screened in a cohort of seven *KAL1*, *FGFR1*, *PROK2* and *PROKR2*

Table 1. Clinical characteristics of all patients and results of *CHD7* analysis[a]

No.	Sex	Diagnosis	Additional features	Family	Mutation CHD7	Parents	MLPA performed
1	M	KS	Dental agenesis, high-arched palate, unilateral perceptive deafness and short stature	Sp	c.8803G>T; p.Glu2935X; exon 38	*De novo*	−
2	M	KS	Cleft palate, auricular dysplasia, nystagmus, bilateral perceptive deafness and hypoplasia of semicircular canals	Sp	c.6347T>A; p.Ile2116Asn; exon 31	*De novo*	−
3	F	KS		Sp	−		−
4	F	KS		Sp	−		−
5	M	KS	High-arched palate	Sp	−		−
6	M	KS	Ptosis	Sp	−		−
7	M	KS		Sp	−		−
8	F	KS	Facial nerve palsy, bilateral colobomas, cleft lip/palate, deafness, short stature and developmental delay	Sp	c.6070C>T; p.Arg2935X; exon 30	*De novo*	−
9	F	KS		Fam	−		+
10	M	KS		Fam	−		−
11	F	KS	Crohn's disease, syndactyly	Fam	−		−
12	M	KS		Fam	−		−
13	M	KS		Sp	−		+
14	F	KS		Sp	−		−
15	F	KS,	Choanal atresia	Fam	−		+
16	M	KS		Fam	−		−
17	M	KS	Congenital deafness and Hirschsprung's disease	Sp	−		−
18	F	KS		Fam	−		−
19	M	KS		Fam	−		−
20	F	KS		Fam	−		+
21	F	KS	Hearing impairment	Fam	−		−
22	M	KS	Deafness	Sp	−		−
23	F	KS	Multiple cranial nerve abnormalities	Sp	−		+
24	F	KS		Fam	−		−
25	F	KS		Sp	−		+
26	M	KS		Fam	−		−
27	M	KS	Hearing impairment	Sp	−		−
28	M	KS		Fam	−		−
29	M	KS		Fam	−		−
30	M	KS	Cryptorchidism	Fam	−		−
31	M	KS		Fam	−		−
32	F	KS	Narrow palate	Fam	−		−
33	F	KS	High-arched palate and hyperlaxity of hand joints	Fam	−		−
34	M	KS	Macrocephaly, hypertelorism, high-arched palate, ataxia, Dandy Walker malformation and developmental delay	U	−		−
35	M	KS		Fam	−		−
36	M	Partial KS	Spinal muscular atrophy	Sp	−		−
37	M	IHH, KS in family	Cardiac septum defect	Fam	−		+
38	M	IHH, KS in family	Hearing impairment	Fam	−		+
39	M	IHH, KS in family		Fam	−		−
40	F	IHH		Fam	−		+
41	M	IHH		Sp	−		+
42	F	IHH	Cardiac septum defect	Sp	−		+
43	M	IHH	Cryptorchidism	Fam	−		−
44	M	IHH	Growth hormone deficient	Fam	−		−
45	F	IHH		Fam	−		−
46	F	IHH		Fam	−		−
47	M	IHH	Cryptorchidism, blind, seizures, mental retardation and short stature	Sp	−		−
48	F	IHH		Fam	−		−
49	M	IHH	Ataxia	Sp	−		−
50	F	IHH		Fam	−		−
51	F	IHH		Fam	−		−

Table 1. Continued

No.	Sex	Diagnosis	Additional features	Family	Mutation CHD7	Parents	MLPA performed
52	M	IHH		Fam	–		–
53	M	IHH		Fam	–		–
54	M	IHH	Developmental delay and high-arched palate	Fam	–		–
55	M	IHH		Fam	–		–
56	F	IHH		Fam	–		–

F, female; Fam, familial; IHH, idiopathic hypogonadotropic hypogonadism; KS, Kallmann syndrome (IHH + anosmia); M, male; MLPA, multiplex ligation probe amplification; partial KS, patient with IHH and anosmia, with some degree of spontaneous pubertal development; Sp, sporadic; U, unknown.
aPatients 1–7 are of Japanese descent and patients 8–56 are from North America.

negative patients of Japanese descent (five males, two females). All had hypogonadotropic hypogonadism and anosmia, whereas some had additional symptoms. Their clinical features are summarized in Table 1, and patient 2 is shown in Fig. 1.

In two of the seven patients, a heterozygous mutation in CHD7 was identified: one nonsense mutation (c.8803G>T; p.Glu2935X) and one missense mutation (c.6347T>A; p.Ile2116Asn). The mutations were proven to be de novo in both patients and were not present in 600 alleles of healthy controls.

The study cohort was extended by 49 North American patients (28 males, 21 females), including 29 patients with KS and 20 with nIHH of whom three had a positive family history for KS. Some of these patients had additional phenotypic features (Table 1). In one of the patients (patient 8), a de novo pathogenic nonsense mutation in CHD7 was found (c.6070C>T; p.Arg2935X).

As whole exon deletions or duplications will be missed by sequence analysis, we performed MLPA analysis. Due to a limited amount of available DNA, we were only able to finish this analysis in 11 patients. Two patients with a relatively high suspicion for CHARGE syndrome based on the features choanal atresia and multiple cranial nerve anomalies (respectively, patient 15 and 23; Table 1) were among those 11 patients. No exon copy number alterations were found.

The main features of the three patients carrying a mutation in CHD7 are given in Table 1. All three patients were proven to be anosmic by formal smell tests. Audiometry revealed a left-sided hearing impairment of 70 dB in patient 1, a bilateral hearing impairment of 60–90 dB in patient 2 and left-sided complete sensorineural deafness and right-sided partial conductive hearing impairment in patient 8. Patient 1 had agenesis of four permanent teeth, the first upper and lower molars. No choanal atresia or heart defects were present in patients 1, 2 and 8. Colobomas were present in patient 8 but excluded by fundoscopy in patients 1 and 2. Patient 2 experienced feeding difficulties during infancy, but these were ascribed to the cleft palate. The dysmorphisms of the ears of patient 2 are very characteristic for CHARGE syndrome with absence of the earlobe and the lower helical fold, and a typical triangular concha (Fig. 1). After identification of the CHD7 mutation, a CT scan of the os petrosum showed bilateral hypoplasia of the semicircular canals. In patients 1 and 8, imaging studies of the temporal bones were not possible. Upon re-evaluation, patient 8 has not only deafness and bilateral colobomas but also left-sided facial nerve palsy, cleft lip and palate, short stature and developmental delay.

In retrospect, patients 2 and 8 have typical CHARGE syndrome according to the commonly used clinical criteria (9), while patient 1 has only some features of this syndrome.

Fig. 1. Lateral view of patient 2. Note the dysmorphic ears with absence of the earlobe and the lower helical fold, and a triangular concha. These dysmorphism are typical for CHARGE syndrome.

Discussion

Hypogonadotropic hypogonadism is a frequent feature in CHARGE syndrome. Chalouhi et al. tested the olfactory function of 14 children with CHARGE syndrome and showed that all children had some degree of olfactory deficiency (14). Pinto et al. showed that olfactory deficiency and abnormal olfactory bulbs were present in all 18 CHARGE syndrome patients in their cohort (15).

These observations prompted us to analyze the *CHD7* gene in 36 patients with KS and 20 patients with nIHH lacking mutations in *KAL1*, *FGFR1*, *PROK2* and *PROKR2*. *CHD7* mutations were identified by sequence analysis in 2 of 7 Japanese KS patients and in 1 of 49 KS/nIHH North American patients. By routine sequencing of the *CHD7* gene, we may have missed mutations located deep in introns or in the promoter region. Furthermore, MLPA analysis could not be performed in all patients.

Hypogonadism in KS is caused by GnRH deficiency. GnRH neurons of the forebrain are thought to originate from the nasal placode. During embryonic development, they migrate alongside the olfactory axons toward the hypothalamus. Mutations in *KAL1*, *FGFR1*, *PROKR2* and *PROK2* can result in hypogonadotropic hypogonadism and anosmia. Therefore, the protein products of these genes are thought to be involved in this combined migration process (8, 19). Because hypogonadotropic hypogonadism and anosmia are frequently present in CHARGE syndrome as well, it is possible that the same embryonic migration process is disturbed in CHARGE syndrome. *CHD7* encodes a protein of the chromodomain (chromatin organization modifier) family. This family shares a unique combination of functional domains consisting of two N-terminal chromodomains, followed by a SWI2/SNF2-like ATPase/-helicase domain and a DNA-binding domain. It is assumed that *CHD* protein complexes affect chromatin structure and gene expression and thereby play important roles in regulating embryonic development (20). Therefore, one might speculate that *CHD7* has a possible influence on the expression or actions of *KAL1*, *FGFR1*, *PROK2* and/or *PROKR2* during development. However, because mutations in these genes account for only 30% of all KS cases, it is possible that *CHD7* impacts on other yet undiscovered, KS genes.

We identified a *de novo CHD7* mutation in three patients initially diagnosed with KS. The two nonsense mutations are known to be pathogenic. The missense mutation p.Ile2116Asn is not located in one of the known protein domains of the CHD7

protein, but it concerns a drastic amino acid change that has not been detected in over 600 control alleles. Furthermore, the p.Gly2108Arg mutation has been shown to be associated with CHARGE syndrome in two families with a variable phenotype, indicating that this part of the protein probably has an important function (12). This indicates that the p.Ile2116Asn mutation is possibly pathogenic.

In retrospect, two of the three *CHD7*-positive patients (patients 2 and 8) had typical CHARGE syndrome with the presence of at least three major features (9). Patient 1 presented with only two additional CHARGE features (short stature and unilateral hearing impairment), although one should notice that vestibular function was not tested in this patient.

From this study, we conclude that it is important to evaluate patients with hypogonadotropic hypogonadism and anosmia for clinical features characteristic of CHARGE syndrome. All three patients were proven to be anosmic. Therefore, the chance to find a *CHD7* mutation seems higher in anosmic patients although the study group is too small to conclude that *CHD7* mutations cannot occur in patients with normosmic IHH. Indeed some patients with CHARGE syndrome are able to smell (personal observations). Because all three patients suffered from hearing impairment, it is tempting to regard this feature as discriminating. However, sensorineural hearing impairment is also an associated feature in males with *KAL1* mutations. Thus, hearing abnormalities may be a sensitive but not very specific symptom of *CHD7* mutations. Hypoplasia or aplasia of the semicircular canals is a much more consistent feature in CHARGE syndrome, even in mildly affected patients (9, 12). Therefore, history taking regarding balance disturbances and gross motor development might reveal indicative information for the presence of a *CHD7* mutation. Abadie et al. have described a specific pattern of postural behavior related to vestibular anomalies in CHARGE syndrome. They noticed a frequent inability to crawl on all fours without resting the head on the floor (5-point crawl), a prolonged duration of standing with support stage and an inability to ride a bike without stabilizers (21). After the first years of life, balance disturbances may not be unequivocally present as a result of visual compensation. In these patients, disequilibrium in the dark is a helpful indication of vestibular deficit. If there is doubt about the vestibular function, screening for vestibular areflexia or imaging of the semicircular canals will be helpful. In the newborn, agenesis of the semicircular canals can be visualized on plain profile X-ray of the

skull (9). In older patients, computerized tomo-graphy or MRI is necessary.

Finally, dilated fundus examination can be per-formed to reveal an optic disc coloboma. A less invasive, but of course also less accurate method, would be to ask for the presence of an optic field defect.

CHD7 screening in the large North American cohort revealed only one mutation. In general, these patients underwent a more extensive clinical work-up (5). From this cohort, we learned that it is not useful to screen the *CHD7* gene in each patient diagnosed with KS or nIHH; additional CHARGE features should be present. Such additional features do not imply that a *CHD7* mutation will be present as has been demonstrated by patient 15 who has choanal atresia but no *CHD7* mutation.

The patients carrying a mutation in *CHD7* in this cohort and the mild *CHD7*-positive patients reported by us in a previous study (12) show that the current diagnostic criteria cannot always dis-criminate between patients with and without a mutation in *CHD7* (9, 12).

We conclude that it is useful to screen patients with hypogonadotropic hypogonadism and anos-mia for clinical features consistent with CHARGE syndrome, particularly hearing impairment, ves-tibular dysfunction and dysmorphisms of the ears. If additional features of CHARGE syndrome are present, *CHD7* sequencing is recommended.

Informed consent

All patients or their legal representatives gave informed consent for the DNA studies and the collection of clinical data. The studies were approved by the institutional review boards. Additional informed consent for publication was obtained of the patient represented by his photo-graph in this manuscript.

References

1. Kallmann FJ, Schoenfeld WA, Barrera SE. The genetic aspects of primary eunuchoidism. Am J Ment Defic 1944: 48: 203–236.
2. Franco B, Guioli S, Pragliola A et al. A gene deleted in Kallmann's syndrome shares homology with neural cell adhesion and axonal path-finding molecules. Nature 1991: 353: 529–536.
3. Legouis R, Hardelin JP, Levilliers J et al. The candidate gene for the X-linked Kallmann syndrome encodes a protein related to adhesion molecules. Cell 1991: 67: 423–435.
4. Dode C, Levilliers J, Dupont JM et al. Loss-of-function mutations in FGFR1 cause autosomal dominant Kallmann syndrome. Nat Genet 2003: 33: 463–465.
5. Pitteloud N, Meysing A, Quinton R et al. Mutations in fibroblast growth factor receptor 1 cause Kallmann syndrome with a wide spectrum of reproductive pheno-types. Mol Cell Endocrinol 2006: 254–255: 60–69.
6. Dode C, Teixeira L, Levilliers J et al. Kallmann syndrome: mutations in the genes encoding prokineticin-2 and prokineticin receptor-2. PLoS Genet 2006: 2: 175.
7. Pitteloud N, Zhang C, Pignatelli D et al. Loss-of-function mutation in the prokineticin 2 gene causes Kallmann syndrome and normosmic idiopathic hypogonadotropic hypogonadism. Proc Natl Acad Sci U S A 2007: 104: 17447–17452.
8. Kim SH, Hu Y, Cadman S, Bouloux P. Diversity in fibro-blast growth factor receptor 1 regulation: learning from the investigation of Kallmann syndrome. J Neuroendocrinol 2008: 20: 141–163.
9. Sanlaville D, Verloes A. CHARGE syndrome: an update. Eur J Hum Genet 2007: 15: 389–399.
10. Vissers LE, van Ravenswaaij CM, Admiraal R et al. Mutations in a new member of the chromodomain gene family cause CHARGE syndrome. Nat Genet 2004: 36: 955–957.
11. Jongmans MC, Admiraal RJ, van der Donk KP et al. CHARGE syndrome: the phenotypic spectrum of muta-tions in the CHD7 gene. J Med Genet 2006: 43: 306–314.
12. Jongmans MC, Hoefsloot LH, van der Donk KP et al. Familial CHARGE syndrome and the CHD7 gene: a recurrent missense mutation, intrafamilial recurrence and variability. Am J Med Genet A 2008: 146: 43–50.
13. Lalani SR, Safiullah AM, Fernbach SD et al. Spectrum of CHD7 mutations in 110 individuals with CHARGE syndrome and genotype-phenotype correlation. Am J Hum Genet 2006: 78: 303–314.
14. Chalouhi C, Faulcon P, Le Bihan C, Hertz-Pannier L, Bonfils P, Abadie V. Olfactory evaluation in children: application to the CHARGE syndrome. Pediatrics 2005: 116: 81–88.
15. Pinto G, Abadie V, Mesnage R et al. CHARGE syndrome includes hypogonadotropic hypogonadism and abnormal olfactory bulb development. J Clin Endocrinol Metab 2005: 90: 5621–5626.
16. Ogata T, Fujiwara I, Ogawa E, Sato N, Udaka T, Kosaki K. Kallmann syndrome phenotype in a female patient with CHARGE syndrome and CHD7 mutation. Endocr J 2006: 53: 741–743.
17. Sato N, Katsumata N, Kagami M et al. Clinical assessment and mutation analysis of Kallmann syndrome 1 (KAL1) and fibroblast growth factor receptor 1 (FGFR1, or KAL2) in five families and 18 sporadic patients. J Clin Endocrinol Metab 2004: 89: 1079–1088.
18. Bergman JE, de Wijs I, Jongmans MC, Admiraal RJ, Hoefsloot LH, van Ravenswaaij-Arts CM. Exon copy

number alterations of the *CHD7* gene are not a major cause of CHARGE and CHARGE-like syndrome. Eur J Med Genet 2008: 61: 417–426.

19. Oliveira LM, Seminara SB, Beranova M et al. The importance of autosomal genes in Kallmann syndrome: genotype-phenotype correlations and neuroendocrine characteristics. J Clin Endocrinol Metab 2001: 86: 1532–1538.

20. Higgs DR, Vernimmen D, Hughes J, Gibbons R. Using genomics to study how chromatin influences gene expression. Ann Rev Genomics Hum Genet 2007: 8: 299–325.

21. Abadie V, Wiener-Vacher S, Morisseau-Durand MP et al. Vestibular anomalies in CHARGE syndrome: investigations on and consequences for postural development. Eur J Pediatr 2000: 159: 569–574.
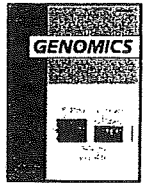
Identification of the mouse paternally expressed imprinted gene *Zdbf2* on chromosome 1 and its imprinted human homolog *ZDBF2* on chromosome 2

Hisato Kobayashi [a,1], Kaori Yamada [a,1], Shinnosuke Morita [a], Hitoshi Hiura [a], Atsushi Fukuda [a], Masayo Kagami [b], Tsutomu Ogata [b], Kenichiro Hata [c], Yusuke Sotomaru [d], Tomohiro Kono [a,*]

[a] *Department of BioScience, Tokyo University of Agriculture, 1-1-1 Sakuragaoka, Setagaya-ku, Tokyo 156-8502, Japan*
[b] *Department of Endocrinology and Metabolism, National Research Institute for Child Health and Development, 2-10-1 Okura, Setagaya-ku, Tokyo 157-8535, Japan*
[c] *Department of Maternal-Fetal Biology, National Research Institute for Child Health and Development, 2-10-1 Okura, Setagaya-ku, Tokyo 157-8535, Japan*
[d] *Natural Science Center for Basic Research and Development, Hiroshima University, 1-2-3 Kasumi, Minami-ku, Hiroshima 734-8551, Japan*

ARTICLE INFO

ABSTRACT

In mammals, both the maternal and paternal genomes are necessary for normal embryogenesis due to parent-specific epigenetic modification of the genome during gametogenesis, which leads to non-equivalent expression of imprinted genes from the maternal and paternal alleles. In this study, we identified a paternally expressed imprinted gene, *Zdbf2*, by microarray-based screening using parthenogenetic and normal embryos. Expression analyses showed that *Zdbf2* was paternally expressed in various embryonic and adult tissues, except for the placenta and adult testis, which showed biallelic expression of the gene. We also identified a differentially methylated region (DMR) at 10 kb upstream of exon 1 of the *Zdbf2* gene and this differential methylation was derived from the germline. Furthermore, we also identified that the human homolog (*ZDBF2*) of the mouse *Zdbf2* gene showed paternal allele-specific expression in human lymphocytes but not in the human placenta. Thus, our findings defined mouse chromosome 1 and human chromosome 2 as the loci for imprinted genes.

© 2009 Elsevier Inc. All rights reserved.

Introduction

Genomic imprinting is an epigenetic gene-marking phenomenon in mammals, which leads to parent-of-origin-dependent monoallelic expression of certain genes, termed imprinted genes [1]. To date, approximately 80 imprinted genes have been identified in mice, the majority of which are present in 11 clusters including the Prader–Willi syndrome/Angelman syndrome and Beckwith–Wiedemann syndrome clusters. These clusters were assigned to 8 autosomal chromosomes, 2, 6, 7, 9, 11, 12, 15, and 17; whereas many solo imprinted genes have been identified on 5 chromosomes (numbers 2, 10, 14, 18, and 19). Many of these imprinted genes with expression patterns were well-conserved between mice and humans. These genes play an important role in fetal growth, development of particular somatic lineages, maternal behavior, tumorigenesis, and birth defects (MRC Mammalian Genetics Unit, Harwell, UK, http://www.mgu.har.mrc.ac.uk/research/imprinting/function.html).

Gene imprinting is initiated by epigenetic modifications such as DNA methylation that occur in the parental germline. In mammals, DNA methylation occurs exclusively at the cytosine residues within cytosine-guanine (CpG) dinucleotides, which plays an important role in normal development [2]. Indeed, many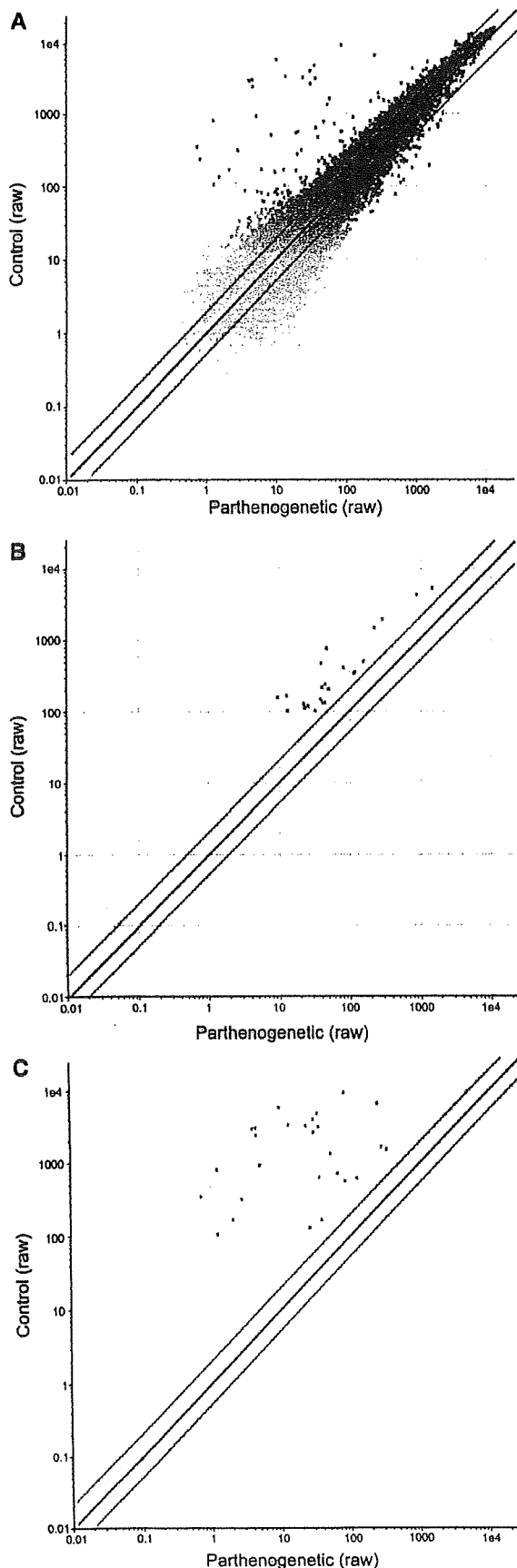 imprinted genes have differentially methylated regions (DMRs), which exhibit parent-of-origin-dependent DNA methylation patterns. Some DMRs function as cis-acting imprinting control regions (ICRs) that exert a regional control on gene expression from an imprinted cluster. Knockout mice studies demonstrated that the de novo DNA methyltransferase Dnmt3a and its related protein Dnmt3L are required to establish the methylation imprints in both maternal and paternal germlines [3–5]. The maintenance methyltransferase Dnmt1 is then required to maintain the differential methylation and imprinted expression patterns in the embryo proper [6,7].

A number of studies have suggested that imprinted genes may have characteristic structural features. For example, it was reported that imprinted genes tend to have fewer and smaller introns [8]. Other reports have described that human and mouse imprinted gene regions contain a lower density of short interspersed transposable elements (SINEs) than non-imprinted regions [9,10]. Thus far, the presence of direct repeats near or within the DMRs has been identified as the potential feature of these regions [11]. However, these features are not observed with regard to all imprinted regions, and their functional relevance is controversial. In a previous study, the dimensions of 15 DMRs (12 maternally imprinted genes and 3 paternally imprinted genes) were measured, and it was revealed that paternally methylated DMRs contain fewer CpGs than maternally methylated DMRs [12]. Furthermore, a recent study has demonstrated that the Dnmt3a/Dnmt3L complex could preferentially methylate CpG site pairs that are 8–10 base pairs apart, and a similar periodicity was observed for the frequency of CpG sites in the 12 maternally imprinted regions [13].

* Corresponding author. Fax: +81 354772543.
  E-mail address: tomohiro@nodai.ac.jp (T. Kono).
¹ These authors contributed equally to this work.

However, no other consensus sequence has been identified for DMRs, and the features that cause them to get preferentially methylated via the Dnmt3a/Dnmt3L complex in the germline remain unknown.

After the first imprinted gene, *Igf2*, was identified in a knockout study, many other methods have subsequently been used to identify imprinted genes in mice. In 1994, *U2afbp-rs* (*Zrsr1*) [14] and *Rasgrf1* [15] were identified as paternally expressed genes with the use of methylation-sensitive restriction enzyme sites as the restriction landmark in the restriction landmark genomic scanning (RLGS) method for screening methylated sites. Subsequently, Ishino's group identified 2 paternally expressed genes, namely, *Peg1* (*Mest*) and *Peg3*, and 2 maternally expressed genes, *Meg1* (*Grb10*) and *Meg3*, by comparison analysis of gene expression among in vitro fertilized parthenogenetic (containing only maternally derived chromosomes) and androgenetic (containing only paternally derived chromosomes) embryos, by suppression subtractive hybridization [16–19]. In 1997, the paternally expressed gene *Impact* was identified using allelic message display without positional cloning or production of parthenogenetic and androgenetic embryos [20]. Furthermore, the development of DNA microarray technology facilitated the identification of many imprinted genes by gene expression profiling. In 2000, Affymetrix GeneChip was used with in vitro fertilized and parthenogenetic embryos and, in 2002, RIKEN cDNA Microarray was used with parthenogenetic and androgenetic embryos to identify new imprinted genes [21,22]. Further, in 2006, Affymetrix GeneChip was used with uniparental disomies [23]. Recently, the imprinted *Mcts2* gene was identified using the sequence features of imprinted genes [24], indicating that bioinformatics analysis can contribute to the identification of novel imprinted genes. Although a recent study has estimated that there are 600 imprinted genes in mice [25], a complete global analysis for locating imprinted genes has not been performed. To elucidate the biological importance of genomic imprinting and other characteristics of imprinted genes, it is important to systematically identify the remaining imprinted genes.

In this study, we compared the gene expression profiles between parthenogenetic and in vitro fertilized embryos (control) by using the Affymetrix GeneChip probe array to identify novel imprinted genes. The control embryos containing both the maternal and paternal genomes exhibited normal expression patterns of both maternally and paternally expressed genes; however, the parthenogenetic embryos that contain 2 maternal genomes exhibited a significantly decreased expression of paternally expressed genes. On the basis of this information, we screened the imprinted gene candidates and confirmed the imprinted expression of these genes by using reverse transcriptase-polymerase chain reaction (RT-PCR) analysis. From this screening, we identified a paternally expressed imprinted gene, *Zdbf2*, on mouse chromosome 1. We also identified a DMR in the paternal allele methylated at 10 kb upstream of the predicted exon 1 of the *Zdbf2* gene. Furthermore, we demonstrated that the human homolog *ZDBF2*, which is mapped to chromosome 2, is also paternally expressed. The newly identified imprinted genes provide an opportunity to further investigate the function and mechanisms of the genomic imprinting machinery.

Results

Screening for new imprinted gene candidates by microarray analyses

In this study, we compared the global expression profiles of mouse parthenogenetic and in vitro fertilized (control) embryos by using the

Table 1
Genes identified by microarray analysis between the control and parthenogenetic embryos

Control	Systematic	GenBank accession	Common name	Fold change	Control		Parthenogenetic		Chromosome
					Raw	Normalized	Raw	Normalized	
<500 raw	1423294_at	AW555393	Mest	96	9196.1	1	84.2	0.01	6
	1448152_at	NM_010514	Igf2	28.4	6508.5	1.01	253.6	0.04	7
	1426208_x_at	AF147785	Plagl1	97.3	5727.5	0.97	9.8	0.01	10
	1421144_at	NM_023879	Rpgrip1	5.5	5316.2	0.97	1460.6	0.18	14
	1433924_at	BM200248	Peg3	84.9	4702.7	1.02	34.5	0.01	7
	1425966_x_at	D50527	Ubc	5.5	4289.8	0.96	884.1	0.17	5
	1417355_at	AB003040	Peg3	88.2	3949.5	1.02	30	0.01	7
	1423506_a_at	AV218841	Nnat	97.7	3321.8	0.98	13.4	0.01	2
	1435383_x_at	AW743020	Ndn	90.5	3216.6	1.03	23.6	0.01	7
	1435382_at	AW743020	Ndn	78.7	3115.9	1.03	36	0.01	7
	1455792_x_at	AV124445	Ndn	99.6	2982	1	4.5	0.01	7
	1415923_at	NM_010882	Ndn	100.2	2871.3	1	4	0.01	7
	1437853_x_at	BB074430	Ndn	81.9	2585.1	1	30.3	0.01	7
	1417356_at	AB003040	Peg3	102.9	2394.6	1.03	4.6	0.01	7
	1417184_s_at	BC027434	Hbb-b1	7	1944	1.01	286.3	0.14	7
	1449939_s_at	NM_010052	Dlk1	6.5	1668.7	1.07	291.2	0.17	12
	AFFX-18SRNAMur/X00686_5_at	AFFX-18SRNAMur/X00686_5	Plgt[a]	8.9	1622	2.33	56.9	0.26	2
	1417714_x_at	NM_008218	Hba-a1	7.6	1470.9	1.15	222.8	0.15	11
	1415896_x_at	NM_013670	Snrpn	28	1336	1.01	53.4	0.04	7
	1435716_x_at	AI836293	Snrpn	102.7	916.7	1.04	5.1	0.01	7
	1421063_s_at	NM_033174	Snrpn	104.8	807.3	1.05	1.2	0.01	7
	1451058_at	AV017653	Mcts2	17.6	766.6	1.04	46.9	0.06	2
	1428111_at	AK003626	Slc38a4	16.9	710.8	1.01	67.8	0.06	15
	1448889_at	NM_027052	Slc38a4	31.6	629.1	1	36.6	0.03	15
	1415911_at	NM_008378	Impact	5.2	618.1	0.94	127.6	0.18	18
	1420688_a_at	NM_011360	Sgce	8.3	558.6	1.04	86.6	0.13	6
	1457356_at	BI793602	Airn	33.4	550	1	20.5	0.03	17
	1457781_at	BG063584	Kcnq1	33.4	537.2	0.97	19	0.03	7
	1455966_s_at	BG070110		5.5	502.8	1.01	156.6	0.18	b
	1458161_at	BM248551	Kcnq1	68.1	500.6	1	8.3	0.01	7
<400 raw	1456783_at	BB075402	9330107J05Rik	14.9	467.5	0.98	39.2	0.07	1
	1427797_s_at	BF580235		5.4	413.9	0.87	80.4	0.16	b
	1437213_at	BG070110		6	411.3	0.98	128.7	0.16	b
<300 raw	1452705_at	AK004611	Pdxdc1	5.5	355.2	0.59	117.4	0.11	16
	1455087_at	AV328498	D7Ertd715e	103	341.8	1.03	0.7	0.01	7
	1445966_at	BG075586	Airn	15	310.6	0.99	22.7	0.07	17
	1456139_at	BM124989	Airn	90.1	309.2	0.97	2.8	0.01	17
<200 raw	1451634_at	BC009123	Airn	19.8	271.1	1.01	19.8	0.05	17
	1427127_x_at	M12573	Hspa1b	5.1	240.5	0.98	45.3	0.19	17
	1436964_at	BB314814	D7Ertd715e	62.9	234.3	0.63	0.8	0.01	7
	1452646_at	AK003956	Trp53inp2	7.6	216	0.95	40.4	0.13	2
	1451386_at	BC027279	Blvrb	6.9	204.3	0.97	49.4	0.14	7
<100 raw	1458179_at	BB526903	Airn	36.6	169	1.01	6.1	0.03	17
	1424010_at	BC022666	Mfap4	16.3	167.1	1.04	12.6	0.06	11
	1450533_a_at	NM_009538	Plagl1	81.4	166.3	0.99	2.1	0.01	10
	1443007_at	AW545941	Gnas	8.9	162	0.94	19	0.11	2
	1439483_at	BI438039	AI506816	12	155.7	0.53	9.4	0.04	b
	1418632_at	BI694835	Ube2h	5.6	147.7	1.01	38.5	0.18	6
	1420978_at	NM_010938	Nrf1	5.1	132.4	0.9	44.6	0.17	6
	1442029_at	BM250850	Kcnq1	68	132.2	0.96	1.5	0.01	7
	1426009_a_at	BC003763	Pip5k1b	6.3	130.1	0.98	42.1	0.15	3
	1417217_at	NM_013779	Magel2	6.3	129.5	0.98	27	0.16	7
	1453164_a_at	AI596401	Ptdss2	9.8	126.2	0.99	22.1	0.1	7
	1453224_at	AW049828	Zfand5	8	117.9	0.99	25.8	0.12	19
	1450383_at	AF425607	Ldlr	5.7	110.3	0.84	23	0.15	9
	1420406_at	NM_013788	Peg12	71.3	105.4	0.97	1.3	0.01	7
	1434952_at	BI734783		5.7	101.8	0.95	32.2	0.17	8
	1429115_at	AK008077	2010003002Rik	9.3	101.7	0.96	13	0.1	4

Genes indicated in bold are known imprinted genes.
[a] Was used as a control gene; therefore, it was excluded from the list of candidate genes.
[b] These sequences matched at more than 2 loci.

Affymetrix GeneChip assay to identify novel imprinted genes. Logically, the expression of an imprinted gene transcribed from the paternally inherited allele will be repressed in parthenogenetic embryos as compared to control embryos. In the microarray analysis, 4 parthenogenetic samples and 4 control samples were hybridized to the GeneChip (Fig. 1A). We used 2 approaches for screening candidates of paternally expressed genes. First, we excluded genes whose raw expression intensities were below 100 in the control embryos, because analysis of genes with low intensities would produce unreliable results. Second, we selected genes whose normalized data in parthenogenetic embryos was more than 5-fold lower than that of control embryos (Table 1). By this screening, we obtained 21 imprinted gene candidates (Fig. 1B), which seemed to be predominantly expressed by paternal allele, excluding 18 known imprinted genes (Fig. 1C). Of the 18 known imprinted genes obtained, 16 genes were known as paternally expressed genes. Therefore, the results of the microarray analysis were reasonable because there is down-regulation of the imprinted genes in parthenogenesis.

Identification of novel imprinted transcripts by RT-PCR

We investigated the polymorphisms in the candidate genes among C57BL/6, DBA/2, and JF1 mice in order to confirm that these candidates are true imprinted genes by allele-specific RT-PCR sequencing analysis. The polymorphism analyses of the candidate genes revealed polymorphisms in a total of 13 candidates: 2 candidates (GenBank accession numbers D50527 and NM_010938) between C57BL/6 and DBA/2 mice, 9 candidates (BB075402, AK004611, BC027279, BI694835, BC003763, AI596401, AF425607, BI734783, and AK008077) between C57BL/6 and JF1 mice, and 2 candidates (NM_008218 and BC027434) among C57BL/6, DBA/2, and JF1 mice (Table 2). To identify the alleles of these genes that were predominantly expressed, we performed RT-PCR sequencing of the candidate genes using BDF1 (C57BL6 × DBA/2), DBF1 (DBA/ 2 × C57BL/6), JBF1 (JF1 × C57BL/6), and BJF1 (C57BL/6 × JF1) mouse embryos at the 9.5-day-old stage (E9.5). All the primer sets for this analysis are listed in Supplemental Table 1. Allele-specific RT-PCR sequencing analysis showed that the BB075402 transcript was expressed only from the paternal allele (Fig. 2).

Expression analysis of mouse Zdbf2—a novel imprinted gene

According to the NCBI Entrez Gene database (http://www.ncbi. nlm.nih.gov/sites/entrez?db=gene), the 655-bp region of the BB075402 sequence corresponded to the 3′-untranslated region (UTR) of the *Zdbf2* (zinc finger, DNA binding factor type containing 2) gene, which contains 7 predicted exons (Fig. 3A). The *Zdbf2* gene was mapped to mouse chromosome 1C2 (Gene ID: 73884). First, we designed 3 specific primer sets (Z1, Z2, and Z3; Z1 primers were used in allele-specific RT-PCR sequencing analysis) for the 3 expressed sequence tags (ESTs) (BB075402, AK033878, and AK015271) that matched the predicted complete *Zdbf2* gene structure in order to confirm the expression levels of the gene (Fig. 3A). Incidentally, the AK033878 transcript (3113 bp) corresponds to the 3′-UTR region of the *Zdbf2* gene, and is registered as a candidate mouse imprinted transcript in the RIKEN database (http://fantom2.gsc.riken.jp/ EICODB/imprinting/). The AK015271 transcript (984 bp) spliced fragment contains exons 1–7 of the *Zdbf2* gene. The microarray assay showed that the BB075402 transcript expression level in the parthenogenetic embryos was 8% (the expression level of the control

was 100%) (Fig. 3B). The results of real-time PCR showed that the expression levels of the BB075402 transcript (Z1) and AK033878 (Z2) in the parthenogenetic embryos were 2% and 3%, respectively (Fig. 3C, D). Furthermore, results of the RT-PCR conducted for the AK015271 transcript (Z3) containing exons 5–7 showed a PCR band in the control embryo, but no such band was detected in the parthenogenetic embryo (Fig. 3E). Thus, we confirmed the repression of the *Zdbf2* gene in parthenogenesis. Second, we designed another primer set (Z4) for the translated region at exon 7 of the *Zdbf2* gene to confirm whether this gene is imprinted. We identified a single nucleotide polymorphism (SNP) in the Z4 region between B6 and JF1 mice. Further, allele-specific RT-PCR sequencing analysis using BJF1 and JBF1 embryos at E9.5 showed that the transcript at the Z4 region was paternally expressed (Fig. 3F). In addition, 5′-rapid amplification of cDNA ends (RACE) analysis of the *Zdbf2* gene, which was performed using BJF1 mouse embryos at E9.5, showed that the expressed transcript almost completely matched exons 1–7 of AK015271; however, exons 1 and 2 were partially matched, and exon 5 was 30 bp longer than that in the transcripts (Supplemental Fig. 1). These results suggest that the mouse *Zdbf2* gene transcript containing at least 7 exons was paternally expressed.

Expression analysis of mouse Zdbf2 in differential developmental stages and tissues

Next, we investigated the *Zdbf2* gene expression pattern in mice during 4 differential developmental stages: 15.5- and 18.5-day-old embryos (E15.5 and E18.5) and 1- and 9-week-old mice. Further, the pattern was investigated by RT-PCR analysis (at Z1 and Z4 regions) of various mouse tissues: the brain, tongue, heart, liver, lung, kidney, and muscle at all ages; the intestine and placenta in only embryos; the spleen in only 1- and 9-week-old mice; and the testis in only 9-week-old adult mice (Fig. 4). Results of the BB075402 (Z1) transcript analysis showed that gene expression was detected in almost all the major tissues from E15.5 and E18.5, except the liver and intestine, which did not show detectable expression in a few cases (Fig. 4A, Supplemental Fig. 1). Furthermore, allele-specific RT-PCR sequencing of BB075402 was performed for all the tissues (strong expression was detected) of BJF1 embryos at E15.5 and 9-week-old adult mice. Interestingly, although almost all the tissues were paternally expressed, placentas from the E15.5 embryos and adult testis exhibited biallelic expression (Fig. 4C,

Table 2
DNA polymorphism information of each paternally expressed candidate gene

Control	Gene	Nucleotide number	C57BL/6	DBA/2	JF1
< 500 raw	NM_023878	a			
	D50527	308	CCCTG	CCTTG	
	BC027434	232, 235	AAGAAAGT	AAAAAGGT	AAAAAGGT
	NM_008218	271	CGGTG	CGCTG	CGCTG
	BG070110	a			
	BB075402	589	TGAAA		TGGAA
< 400 raw	BF580235	a			
< 300 raw	AK004611	772	ACGTA		ACATA
	M12573	a			
< 200 raw	AK003956	a			
	BC027279	263	CCGTC		CCATC
< 100 raw	BC022666	a			
	BI438039	b			
	BI694835	154	TAAGA		TADGA
	NM_010938	1995	GAATG	GAGTG	
	BC003763	1894	GGACC		GGGCC
	AI596401	152	ATAGG		ATTGG
	AW049828	b			
	AF425607	395	CGATG		CGCTG
	BI734783	227	CCCAA		CCDAA
	AK008077	733	CATAG		CAAAG

All polymorphisms are shown in red.
  a No polymorphisms were identified.
  b No PCR bands were detected by RT-PCR.

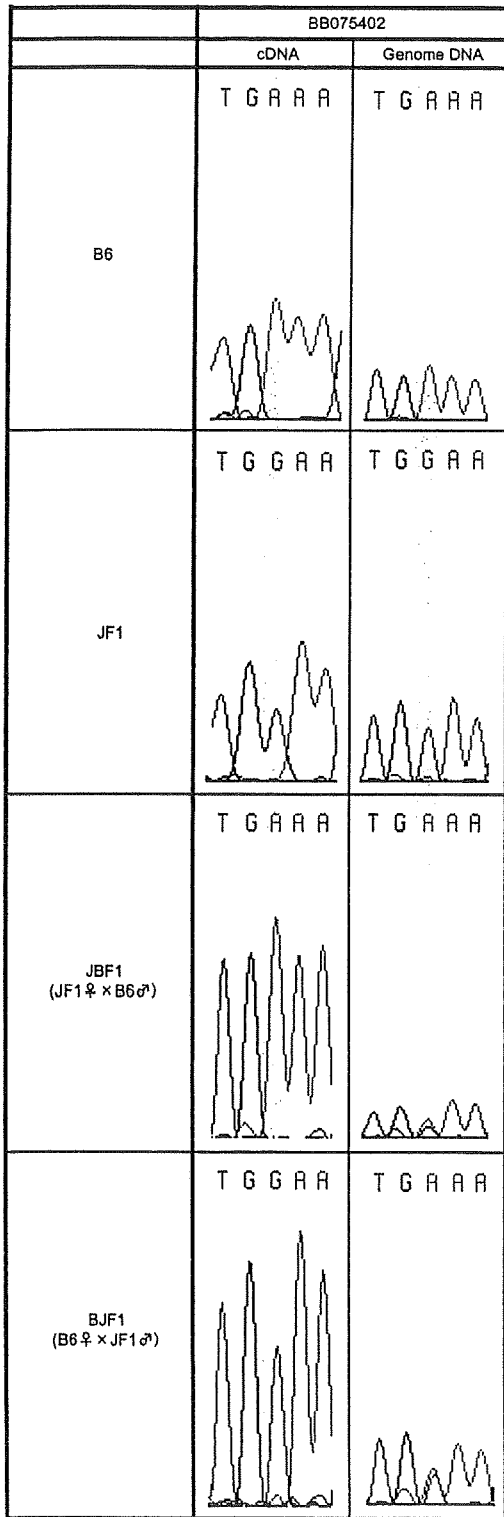|	BB075402	
	cDNA	Genome DNA
B6	T G A A A	T G A A A
JF1	T G G A A	T G G A A
JBF1 (JF1♀ × B6♂)	T G A A A	T G A A A
BJF1 (B6♀ × JF1♂)	T G G A A	T G A A A

Fig. 2. Expression analysis of BB075402. Allele-specific RT-PCR sequencing analysis of BB075402 was performed with C57BL/6 (B6), JF1, BJF1, and JBF1 mouse embryos at E9.5 (n = 3). The SNP of BB075402 is highlighted in yellow.

Supplemental Fig. 2). Meanwhile, expression at the Z4 region was detected in the brain, tongue, heart, lung, intestine, kidney, muscle, and placenta in E15.5 embryos and in the brain, tongue, kidney, muscle, and placenta in E18.5 embryos (Fig. 4B). Allele-specific RT-PCR sequencing of

the Z4 region showed similar results to that of BB075402 (data not shown). These results strongly suggested that the transcript of the mouse Zdbf2 gene is paternally expressed in almost all expressed tissues, but is biallelically expressed in only the placenta and testis.

Parent-of-origin-specific methylation of the mouse Zdbf2 gene

Many imprinted genes are epigenetically regulated by epigenetic mechanisms such as DNA methylation. DNA methylation occurs exclusively at cytosine residues within CpG dinucleotides. DMRs have been identified in CpG-rich regions (CpG islands) around imprinted genes in the maternal and paternal genomes, and it has been demonstrated that these regions function as ICRs. To explore and understand the regulation of the imprinted Zdbf2 gene, we analyzed the DNA methylation status by using the bisulfite sequencing method [26].

The genomic DNA sequence of the mouse Zdbf2 gene was derived from the mouse BAC clone RP23-434D24 (GenBank accession number AL669947, Fig. 5A). First, we identified 3 putative CpG islands within the AL669947 sequence using EMBOSS CpGplot (http://www.ebi.ac. uk/emboss/cpgplot/), and termed them CG1, CG2, and CG3 (Fig. 5A). These CpG islands were defined as a 200-bp stretch of DNA with a GC content of over 50% and an observed CpG/expected CpG (Obs/Exp CpG) ratio greater than 0.6. The CG1 region was observed 25 kb upstream of the Zdbf2 gene. CG2 contains the promoter and exon 1 of the Zdbf2 gene. We identified some SNPs in the CG1 and CG3 regions but not in CG2 by direct sequencing of samples from C57BL/6 and JF1 mice (Table 3). The CG3 contains 29 copies of the cytosine-rich 18-bp direct repeat and is included in exon 7 (Supplemental Fig. 3). To examine the differential methylation between paternal and maternal alleles in these CpG islands, we subjected them to bisulfite sequencing analyses for the CG1 and CG3 regions using 9.5-day-old in vitro fertilized embryos (BJF1 mice) and for the CG2 region using 9.5-day-old parthenogenetic and androgenetic embryos. The results showed that all the analyzed regions were almost unmethylated in both the alleles (Fig. 5B–D).

Second, by changing the CpG island criteria (minimum length, 100 bp; GC content, >50%; Obs/Exp CpG, >0.6), we identified a relatively CpG-rich region 10 kb upstream of the Zdbf2 gene, between the CG1 and CG2 regions, and also identified SNPs in this region between C57BL/6 and JF1 mice (Table 3). We performed bisulfite sequence analysis for this region similar to the 3 CpG islands (Fig. 5E). Interestingly, paternal allele-specific methylation was detected in the CpG-rich region. Furthermore, bisulfite sequencing analyses of oocytes and sperms revealed that this region was hypomethylated in oocytes but highly methylated in sperms. These results showed that this CpG-rich region was methylated on the paternal alleles and that the methylation was derived from germline, similar to H19 DMR, Dlk1-Gtl2 IG-DMR, and Rasgrf1 DMR, which are known as paternal methylation imprints [27–29]; thus, we termed this region Zdbf2 DMR.

Human homologous ZDBF2 is paternally expressed in lymphocytes but not in the placenta

Most known imprinted genes have been identified among mammalian species, especially in mice and humans, but species-specific imprinting has been reported in some genes, like Igf2r and Impact [30,31]. To verify the imprinting status of the human homolog ZDBF2, we examined an SNP in the ZDBF2 gene by direct sequencing of cDNA from human tissues. On the basis of the NCBI Entrez human gene database, the human homolog ZDBF2 gene containing 5 exons was mapped to chromosome 2q33.3 (Gene ID: 57683), and no imprinted genes were identified on human chromosome 2. We designed a primer set within the last exon of ZDBF2 (exon 5) including the SNP (reference SNP ID: rs10932150). We then
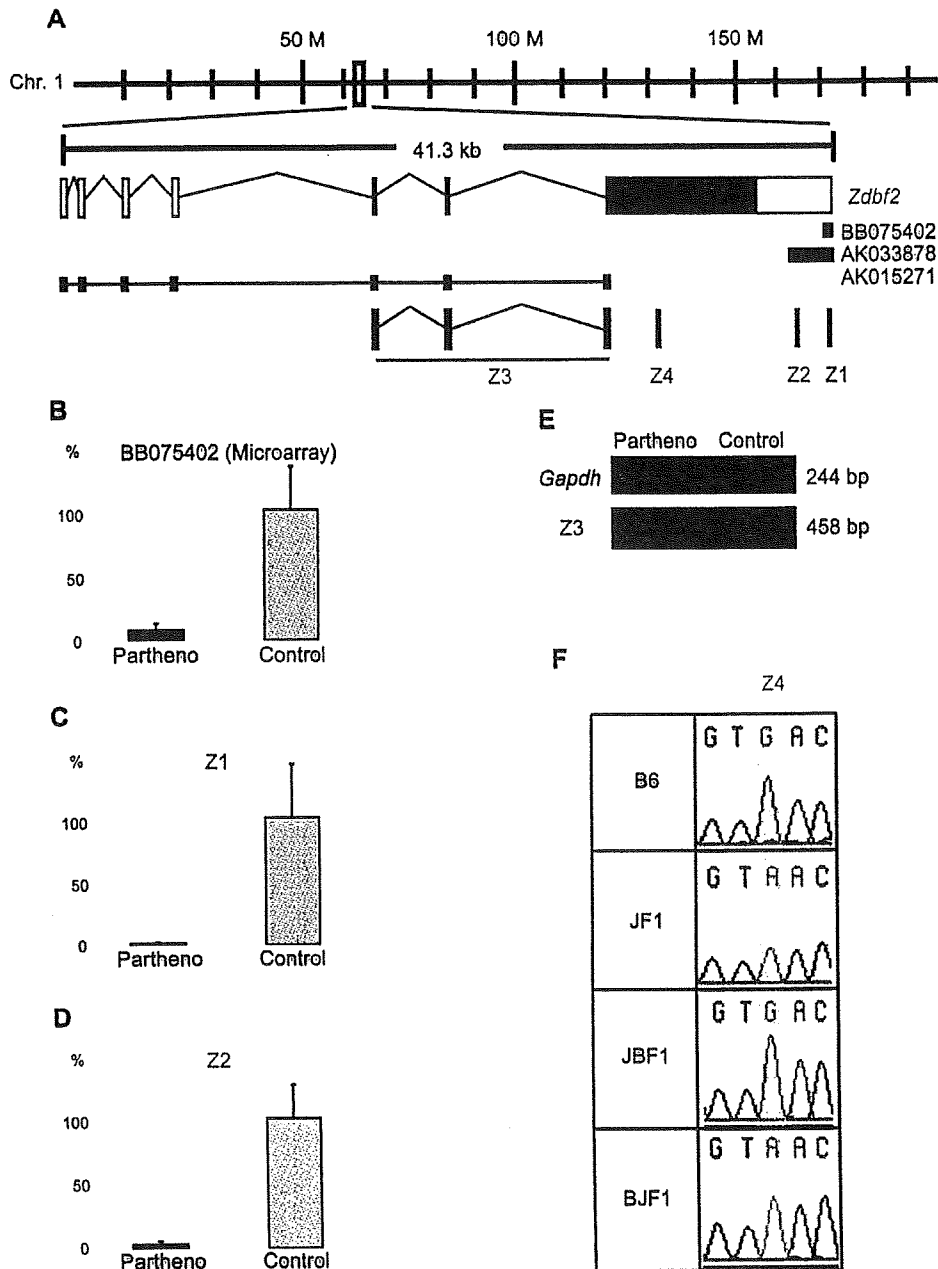
Fig. 3. Expression analysis of a novel paternally expressed gene, *Zdbf2*, on mouse chromosome 1. (A) Map of the *Zdbf2* gene on chromosome 1. Three EST positions and the primer positions of the Z1–Z4 regions are shown in the map. (B) Expression analysis of BB075402 by the microarray method. Partheno: parthenogenetic embryos (n = 4); control: in vitro fertilized control embryos (n = 4). Expression analysis of the Z1 (BB075402) (C) and Z2 regions (AK033878) (D) by real-time RT-PCR in the parthenogenetic (n = 3) and control embryos (n = 3). Values are expressed as mean ± s.e.m. (E) Expression analysis of the Z3 region (AK0152712) by RT-PCR in the control and parthenogenetic embryos. (F) Allele-specific RT-PCR sequencing analysis of the Z4 region with B6, JF1, BJF1, and JBF1 mouse embryos at E9.5 (n = 3). The SNP of Z4 is highlighted in yellow.

performed RT-PCR analysis using human lymphocytes from a child who was heterozygous for a G/A polymorphism at the rs10932150 site, and only allele A from the father was detected (Fig. 6A, B). Furthermore, we examined the SNP in the human placenta, which was also heterozygous and, surprisingly, both G and A alleles were detected (Fig. 6C). These results revealed that the human *ZDBF2* gene is paternally expressed in lymphocytes but biallelically expressed in the placenta. This placenta-specific gene escape from imprinting is similar to that observed in the imprinted mouse *ZDBF2* gene. These results demonstrated that an imprinted locus is present on human chromosome 2.

Discussion

This study aimed to identify novel imprinted genes by comprehensive comparison of mouse gene expression. We successfully identified a imprinted gene, *Zdbf2*, which was mapped to mouse chromosome 1C2, and its imprinted human homolog, *ZDBF2*, which was mapped to human chromosome 2q33.3. The discovery of the imprinted *Zdbf2* gene may provide an opportunity to identify additional imprinted genes in the vicinity of this gene because of the clustering tendency of imprinted genes. Currently, the function of the *Zdbf2/ZDBF2* gene is unknown. Meanwhile, previous studies
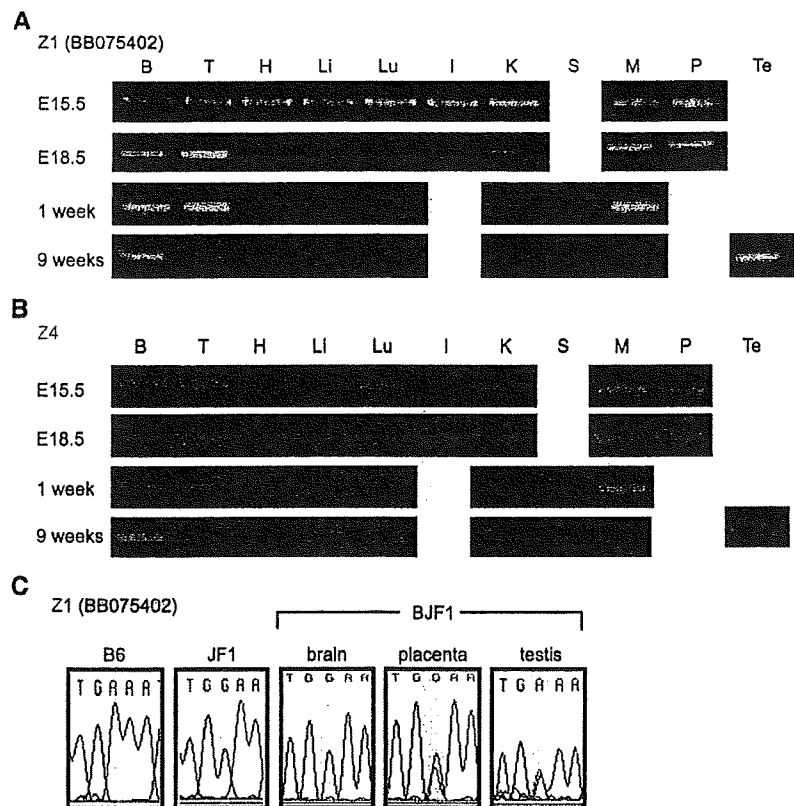
Fig. 4. Stage- and tissue-specific expression of the Zdbf2 gene. Expression analysis by RT-PCR of Z1 (A) and Z4 (B) in the tissues (B = brain, T = tongue, H = heart, Li = liver, Lu = lung, I = intestine, K = kidney, S = spleen, M = muscle, P = placenta, and Te = testis; n = 3, respectively) of BJF1 mouse embryos at 15.5 and 18.5 days (E15.5 and E18.5) and 1- and 9-week-old adult mice (1 week and 9 weeks). (C) Allele-specific RT-PCR sequencing analysis of Z1 (BB075402) using B6 and JF1 mouse embryos at E9.5, the brain and placenta from BJF1 embryos at E15.5, and the testis from adult BJF1 mice (n = 2). The SNP of BB075402 is highlighted in yellow.

reported that maternal and paternal uniparental isodisomies for human chromosome 2 were responsible for various abnormalities [32–35]. Investigating the functions of the Zdbf2 gene and other imprinted genes may provide further information about the imprinting disorders and mechanism.

In this study, we compared gene expression profiles between parthenogenetic and in vitro fertilized embryos (control) using the Affymetrix GeneChip probe array. We obtained 18 known imprinted genes and 21 candidates of paternally expressed genes. Some of the known imprinted genes included paternally expressed genes that were previously identified using subtraction hybridization in 9- to 10-day-old parthenogenetic and control embryos, similar to those used in our study [16,17,21,36], or embryonic fibroblast cell lines [37]. Of the obtained known imprinted genes, Kcnq1 and Gnas are known as maternally expressed genes. These genes were accompanied by a paternally expressed antisense gene (Kcnq1ot1) or an alternative gene form (Gnasxl); therefore, these transcripts might be hybridized to the array [38,39]. Although we obtained several known imprinted genes from this screening, we could not obtain all the known imprinted genes. The reasons may include the decreased detection capability of tissue-specific imprinted gene expression because of RNA isolation from whole embryos or immature organ formation of each sample.

Of the 21 paternally expressed gene candidates, we identified polymorphisms among C57BL/6, DBA/2, and JF1 mice with 13 candidates. We used RT-PCR analysis and identified that of these, the BB075402 transcript was expressed only from the paternal allele. Mean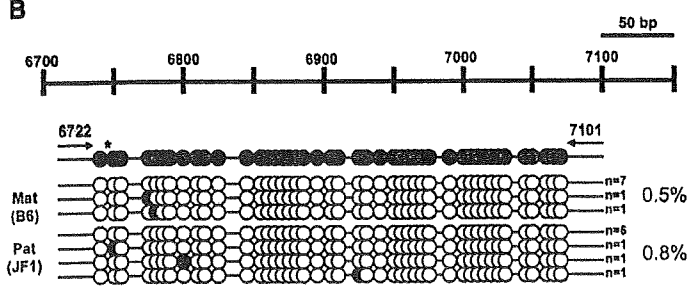while, many paternally expressed gene candidates exhibited biallelic expression in RT-PCR analysis. The differential expression of such genes between parthenogenetic and control embryos could be explained using 2 reasons. First, since 9.5-day-old parthenogenetic embryos exhibited delayed development as compared to the controls at the same stage of development, stage-specific genes might have been selected in this screening. Second, disruption of the imprinted gene expression in parthenogenesis might affect the expression of the non-imprinted genes, which were detected as false imprinted genes. These arguments were described in the discussion section of the previous studies [22,40]. The remaining candidate genes in which no polymorphisms were detected need to be further evaluated to determine whether they are true imprinted genes. Further investigation with other reciprocal crosses would be useful for identifying polymorphisms between the strains.

The BB075402 transcript was registered as a RIKEN mouse EST obtained from adult male diencephalons, and our study demonstrated expression of the BB075402 transcript (Z1 region) in the brain. Though almost all the major tissues showed clear expression of this transcript during embryogenesis, the tissues expressing this gene were limited to the brain, tongue, and muscle, and the testis after birth. The 3'-region of the AK033878 transcript corresponds to the BB075402 transcript, and both transcripts showed decreased expression in parthenogenetic embryos. Moreover, a part of the AK015271 transcript (Z3 region), which contains exons 1–7 of the mouse Zdbf2 gene, was observed to show decreased expression in parthenogenetic embryos as determined by RT-PCR. We could further perform allelic expression analysis on the translated region (Z4 region shown in Fig. 3) of the mouse Zdbf2 gene, and the results revealed that the
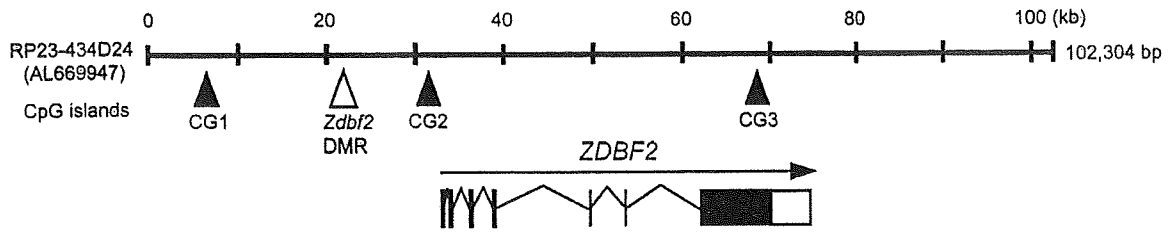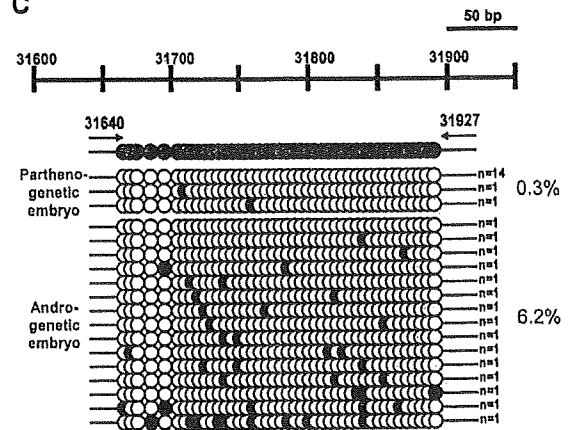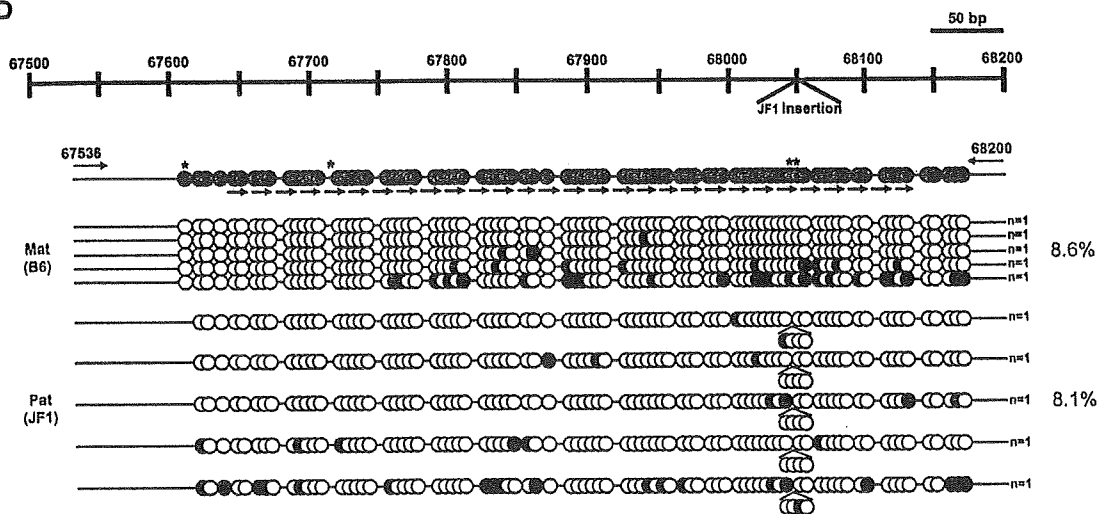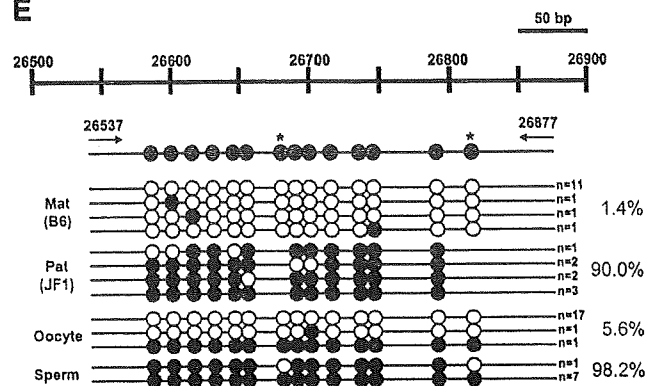
Table 3
DNA polymorphism information on each CpG-rich region surrounding the mouse *Zdbf2*
gene

Region	Nucleotide number (AL669947)	C57BL/6	JF1
CG1	6753	GGAAG	GGGAG
Zdbf2 DMR	26681	CTCGA	CTTGA
	26819	TCCGA	TCTGA
CG2	a		
CG3	67619	GCGCT	GCCCT
	67716	GCCCC	GCACC
	68030	CGCGC	CGGGC
	68053	CC---------------CG	CCCGTGCCCCCGCGCGCCCG

All polymorphisms are shown in red.
a No polymorphisms were identified.

translated region was paternally expressed similar to the BB075402 transcript. These results strongly indicated that these transcripts were the same products expressed solely from the paternal allele. It appeared that exons 5–6 of *Zdbf2* are also paternally expressed; however, it remained unknown as to whether the large (13 kb) transcript of the *Zdbf2* gene is expressed. Therefore, we tested 5'-RACE using mouse embryos at E15.5, and we could confirm that the expressed splice form (exons 1–7) was almost identical to the AK015271 transcript. Meanwhile, Z1 and Z4 primers did not detect expression in all the same tissues. For example, in embryonic liver, expression of the Z1 region was detectable but the Z4 region was not. Though this may be caused by the presence of different forms of the *Zdbf2* transcript in different tissues, to reveal (tissue-specific) splice variants of *Zdbf2* gene is required in future.

According to the database, the mouse *Zdbf2* gene encodes a 2493-amino acid protein with a predicted mass of 270 kDa. In our study, we demonstrated that the human *ZDBF2* gene was paternally expressed in lymphocytes. Furthermore, the human unidentified gene-encoded (HUGE) protein database of the Kazusa DNA Research Institute provides the expression profile of the human *ZDBF2* gene based on RT-PCR and enzyme-linked immuno-sorbent-assay (ELISA) [41]. It is shown that the expression level of this gene in the brain and muscle is higher than that in other tissues such as those in the heart, lung, liver, kidney, pancreas, and spleen (http://www.kazusa.or.jp/huge/gfpage/KIAA1571/). Interestingly, our study showed that mouse *Zdbf2* gene expression was detected in only the brain, tongue, and muscle through the embryo to the adult stages. Thus, the expression profile of human *ZDBF2* was similar to that of mouse *Zdbf2*, which was investigated in our study. Furthermore, analyses of imprinted expression patterns showed that biallelic expression of mouse and human homologs was detected in placental tissues despite the paternal allele-specific expression observed in almost all other tissues (except for the testis) The possibility of placental tissues containing maternal materials was not completely excluded, however, the other imprinted gene (H19) showed normal imprinted expression pattern in both human and mouse placental tisses (data not shown). These facts indicate that the regulation mechanism of *Zdbf2*/*ZDBF2* gene expression is well conserved between mice and humans. Further comparison analyses of *Zdbf2*/*ZDBF2* gene products may provide hints for revealing those functions. For example, additional homologous *Zdbf2* anchors among chimpanzees, rats, dogs, horses, and chickens have been identified (Gene ID: 470622, 501153, 488490, 100068542, and 424100). These facts indicated that this gene plays an evolution-

ally conserved role among at least these organisms. There were no reports of the imprinted genes showed biallelic expression specifically in placenta and testis, like *Zdbf2* gene. By contract, some imprinted genes shows placenta-specific imprinted expression, and one of them, *Mash2*/*Ascl2* gene is essential for placental development [42]. The elucidation of the function of *Zdbf2* gene may explain the reason of the placenta- and testis-specific escape imprinting.

As previously noted, imprinted genes were regulated by parent-of-origin-specific DNA methylation in the DMR in *cis*. On analyzing the DNA methylation status at 4 CpG-rich regions around the mouse *Zdbf2* gene, we identified a paternal allele-specific methylated region, *Zdbf2* DMR, which is 10 kb upstream of the *Zdbf2* gene. Thus far, similar DMRs have been found in only 3 imprinted loci—*H19-Igf2*, *Dlk1-Gtl2*, and *Rasgrf*—and it has been demonstrated that these DMRs function as the ICRs controlling the neighboring imprinted genes. In particular, methylation of *H19* DMR and *Dlk1-Gtl2* IG-DMR acts as paternal methylation imprinting and prevents parthenogenesis [43,44]. Interestingly, 2 paternally expressed genes, *Igf2* and *Dlk1*, were included in the 18 known imprinted genes that were obtained from our microarray screening. This indicates that hypomethylation of *H19* DMR and IG-DMR inhibits paternally expressed genes on both maternal alleles in a parthenogenetic embryo, and that the methylation of *Zdbf2* DMR may also regulate the paternally expressed *Zdbf2* gene and the hitherto undiscovered neighboring imprinted genes. Moreover, the methylation of *Zdbf2* DMR might be established in gonocytes because the other 3 paternal methylation imprints are established in this stage [45–49], but the details of this remain unknown. The regulatory mechanism of the *Zdbf2* gene and the role of DNA methylation at the *Zdbf2* DMR should be clarified. The identification of novel paternally methylated DMRs was important and valuable, because only 3 cases showing such methylation patterns were reported, even though over 10 maternally methylated DMRs were reported. Further characterization of *Zdbf2* DMR is required to demonstrate the mechanisms by which the paternally methylated DMRs were methylated (targeted) by DNA methyltransferases. Although the real role of the repeat element in genomic imprinting [50,51] is still unknown, we identified a direct repeat sequence on the *Zdbf2* gene, similar to the other imprinted genes. In conclusion, we successfully defined mouse chromosome 1 and human chromosome 2 as the imprinted loci. Our findings provide a new platform for further identification of new imprinted genes and new insight into control of parental gene expression.

Materials and methods

Extraction of total RNA from parthenogenetic, androgenetic, and control embryos for microarray analysis

Parthenogenetic and androgenetic embryos were prepared as described previously [52]. Briefly, parthenogenetic embryos were constructed by stimulating unfertilized BDF1 eggs (C57BL6 × DBA/2; Clea Japan, Tokyo, Japan) with strontium chloride solution, which contains cytochalasin B to prevent extrusion of the second polar body. Androgenetic embryos were produced by in vitro fertilization of enucleated oocytes from BDF1 mice. Pronuclear transfer (from male BDF1 mice) was performed to produce diploid androgenetic embryos. Control biparental embryos were produced by the in vitro fertilization of non-manipulated oocytes. These embryos were introduced into an

Fig. 5. Methylation profiles of *Zdbf2* DMR and CpG islands surrounding the mouse *Zdbf2* gene. (A) Genomic structure of the mouse *Zdbf2* gene. The filled vertical arrowheads indicate the positions of each CpG island, i.e., CG1, CG2, and CG3. The open vertical arrowhead indicates the position of the relatively CpG-rich region, i.e., *Zdbf2* DMR. The filled vertical arrowheads indicate the positions of each CpG island—CG1, CG2, and CG3. The methylation status of (B) CG1, (C) CG2, and (D) CG3 in the 9.5-day-old in vitro fertilized (BJF1 mice; n = 2), parthenogenetic, and androgenetic embryos (n = 2). Coordinates are from GenBank Sequence AL669947. The 29 continuous arrows (horizontal) indicate direct repeats within the CG3 region. (E) Methylation of *Zdbf2* DMR in the 9.5-day-old in vitro fertilized (BJF1 mice) embryos, oocytes, and sperm. The open and closed circles indicate methylated and unmethylated CpGs. The asterisks represent polymorphism positions between B6 and JF1 mice. The maternal and paternal alleles were distinguished by polymorphisms, if present, between C57BL6 (B6) and JF1 mice. Mat, maternal (B6) allele; Pat, paternal (JF1) allele. n: number of DNA clones.
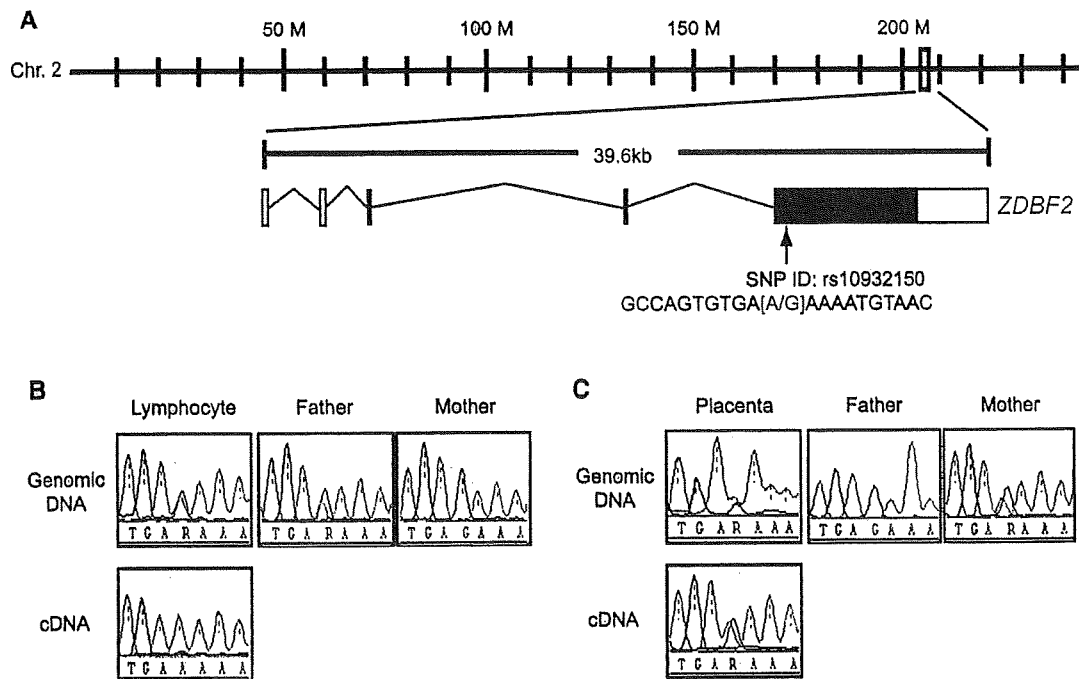
Fig. 6. Expression analysis of the ZDBF2 gene on human chromosome 2. (A) Genomic structure of the human ZDBF2 gene. The arrow indicates the position of the SNP (ID: rs10932150). The SNP sequence is indicated in red. Allele-specific RT-PCR sequencing analysis in (B) the human lymphocyte cell line and (C) placenta. The SNP of exon 5 is highlighted in yellow.

adult CD-1 mouse uterus. The 9.5-, 15.5-, and 18.5-day-old embryos were harvested, and TRIzol (Invitrogen, Carlsbad, CA) was used to extract total RNA from the embryos.

cRNA preparation and microarray hybridization

A 1-µg aliquot of total RNA was used as the template for cDNA synthesis (Eukaryotic Poly-A RNA Control Kit and One-Cycle cDNA Synthesis Kit; Affymetrix, Santa Clara, CA). The cDNA was purified with the Sample Cleanup Module (Affymetrix). Following cleanup, biotin-labeled cRNA was synthesized using the GeneChip IVT Labeling Kit (Affymetrix), and fragmented and purified with the Sample Cleanup Module (Affymetrix). The fragmented cRNA was hybridized with Affymetrix Mouse genome 430 2.0 GeneChip at 45 °C for 16 h. The GeneChips were then washed and stained with a GeneChip Fluidics Station 460 (Affymetrix) according to the Expression Analysis Technical Manual. An Affymetrix GeneChip Scanner 3000 was used to quantify the signal.

Microarray data analyses

The Affymetrix Mouse genome 430 2.0 GeneChip contains 45101 genes and ESTs. We compared the parthenogenetic embryos with control embryos by using the following 3 normalization methods: data transformation, where the set measurements were less than 0.01–0.01; per chip normalization, where the values were normalized to the 50th percentile to limit the range of variation; and per gene normalization, where the values were normalized to specific samples.

Polymorphism analyses among candidate genes

C57BL/6 and DBA/2 mice were purchased from Clea Japan, and JF1 mice [53] obtained from the National Institute of Genetics in Mishima, Japan. Genomic DNA was isolated from the tails of C57BL/6, DBA/2, and JF1 mice by digestion with proteinase K (Invitrogen), which was followed by phenol/chloroform extraction. The DNA was

amplified by PCR with TaKaRa Ex Taq polymerase (TaKaRa, Kyoto, Japan). The primer sequences were complementary to the exon sequences of the candidate genes, and the PCR conditions are listed in Supplemental Table 1. The PCR products were purified with Wizard SV Gel and the PCR Clean-Up System (Promega, Madison, WI). PCR amplification was performed with TaKaRa Ex Taq polymerase. The purified PCR products were sequenced with primers for the direct sequence and the ABI PRISM 3130 Genetic Analyzer (Applied Biosystems, Foster, CA).

RT-PCR and allelic expression analyses among candidate genes

Using TRIzol (Invitrogen), we isolated total RNA from BDF1, DBF1 (DBA/2 × C57BL/6), JBF1 (JF1 × C57BL/6), and BJF1 (C57BL/6 × JF1) embryos at day 9.5. After total RNA was treated with DNase (Promega) to exclude the genomic DNA, the absence of genomic DNA contamination was confirmed by the lack of amplification of GAPDH by PCR. The genomic DNA-free total RNA was reverse transcribed to cDNA with SuperScript II (Invitrogen). The expression of 22 candidate imprinted genes was examined by RT-PCR. The primer sequences and PCR conditions are listed in Supplemental Table 1 and Supplemental Table 2. To investigate the expression patterns of Zdbf2, different tissues at various developmental stages (15.5-, and 18.5-day-old embryos and 1- and 9-week-old mice) were harvested, and TRIzol (Invitrogen, Carlsbad, CA) was used to extract total RNA.

5′-RACE analysis

The 5′-region of the mouse Zdbf2 gene was obtained using the 5′-Full RACE Core Set (TaKaRa). Total RNA was prepared from 9.5-day-old BJF1 embryos, and a Zdbf2 gene-specific 5′-end phosphorylated primer (P2, 5′-ATTCCAAGGACTGCTGCTGT-3′) was used. We performed 2 rounds of PCR by using TaKaRa LA Taq (TaKaRa) under the following conditions: 25 cycles of 30 s at 94 °C, 30 s at 55 °C, and 4 min at 72 °C for the first PCR and 25 cycles of 30 s at 94 °C, 30 s at 60 °C, and 4 min at 72 °C for the second PCR. The primer sets

used for the nested PCR were as follows: Sense S1, 5'-TAGACCTGG-TACTTCTCAGGAACA-3' and anti-sense A1, 5'-CAACAGATCCTGAATCC-TCGGAGT-3' for the first PCR; sense S2, 5'-CACGCAGAAGTTGCAGTTCG-3' and anti-sense A2, 5'-TCTGCACCGCTATCTGCAG-3' for the second PCR. The amplified products were purified and directly sequenced.

DNA methylation analyses

Genomic DNA samples isolated from 9.5-day-old parthenogenetic, androgenetic, and control embryos or from the sperm and oocytes of adult BJF1 mice were treated with sodium bisulfite [26] using the EpiTect Bisulfite Kit (QIAGEN, Valencia, CA). The bisulfite-treated DNA was amplified by PCR with TaKaRa *Ex Taq* Hot Start Version (TaKaRa) for CpG-rich regions around the mouse *Zdbf2* gene. The primers and PCR conditions for the amplification are listed in Supplemental Table 3. The PCR products were subcloned into pGEM-T Easy vector (Promega), which was transformed into DH5α cells. Colonies were selected and transferred into 96-well plates, and DNA was amplified by rolling circle amplification [54] with an Illustra TempliPhi DNA amplification kit (GE Healthcare Bio-Sciences, Little Chalfont, UK). DNA was sequenced using standard primers (SP6, 5'-GATTTAGGTGA-CACTATAG-3' and T7, 5'-TAATACGACTCACTATAGGG-3') and the ABI PRISM 3130 Genetic Analyzer (Applied Biosystems). The percentage of methylation was calculated as the number of methylated CpG dinucleotides from the total number of CpGs at every CpG island (CpG-rich region). At least 5 clones from each region and each parental allele were sequenced.

Expression analysis of human ZDBF2

This study was approved by the Institutional Review Board Committee at National Center for Child Health and Development, and performed after obtaining written informed consent from each subject or his or her parent(s). Genomic DNA was isolated from human lymphocytes with the use of a FlexiGene DNA Kit (Qiagen). Total RNA was extracted from human lymphocyte cell lines with RNeasy Plus Mini Kit (Qiagen), and the total RNA from human placenta was extracted with ISOGEN (Nippon Gene, Tokyo, Japan). The extracted RNA was DNase-treated with deoxyribonuclease (RT Grade) for heat stop (Nippon Gene). DNase-treated RNA was purified by phenol/chloroform extraction. The genomic DNA-free total RNA was reverse transcribed to cDNA with SuperScript III (Invitrogen). PCR carried out in a 50-μl volume reaction mixture containing cDNA (equivalent of 20–50 ng total RNA), 1× PCR buffer, 2.5 U of AmpliTaq Gold (Applied Biosystems), 50 pmol of each primer, and 10 mM dNTPs. The primers used for human *ZDBF2* were 5'-AAACTGGA-GAAGGGACAGCA-3' and 5'-CAAATGAGCTGCTGGTGGTA-3'. The cycling protocol was as follows: 1 min at 94 °C; 30 cycles of 94 °C for 1 min, 57 °C for 1 min, and 72 °C for 1 min; and 5 min at 72 °C.

Acknowledgments

Appendix A. Supplementary data

Supplementary data associated with this article can be found, in the online version, at doi:10.1016/j.ygeno.2008.12.012.

References

[1] W. Reik, J. Walter, Genomic imprinting: parental influence on the genome, Nat. Rev. Genet. 2 (2001) 21–32.

[2] E. Li, T.H. Bestor, R. Jaenisch, Targeted mutation of the DNA methyltransferase gene results in embryonic lethality, Cell 69 (1992) 915–926.

[3] D. Bourc'his, G.L. Xu, C.S. Lin, B. Bollman, T.H. Bestor, Dnmt3L and the establishment of maternal genomic imprints, Science 294 (2001) 2536–2539.

[4] K. Hata, M. Okano, H. Lei, E. Li, Dnmt3L cooperates with the Dnmt3 family of de novo DNA methyltransferases to establish maternal imprints in mice, Development 129 (2002) 1983–1993.

[5] M. Kaneda, et al., Essential role for de novo DNA methyltransferase Dnmt3a in paternal and maternal imprinting, Nature 429 (2004) 900–903.

[6] E. Li, C. Beard, R. Jaenisch, Role for DNA methylation in genomic imprinting, Nature 366 (1993) 362–365.

[7] R. Hirasawa, et al., Maternal and zygotic Dnmt1 are necessary and sufficient for the maintenance of DNA methylation imprints during preimplantation development, Genes Dev. 22 (2008) 1607–1616.

[8] L.D. Hurst, G. McVean, T. Moore, Imprinted genes have few and small introns, Nat. Genet. 12 (1996) 234–237.

[9] J.M. Greally, Short interspersed transposable elements (SINEs) are excluded from imprinted regions in the human genome, Proc. Natl. Acad. Sci. U. S. A. 99 (2002) 327–332.

[10] X. Ke, N.S. Thomas, D.O. Robinson, A. Collins, The distinguishing sequence characteristics of mouse imprinted genes, Mamm. Genome 13 (2002) 639–645.

[11] B. Neumann, P. Kubicka, D.P. Barlow, Characteristics of imprinted genes, Nat. Genet. 9 (1995) 12–13.

[12] H. Kobayashi, et al., Bisulfite sequencing and dinucleotide content analysis of 15 imprinted mouse differentially methylated regions (DMRs): paternally methylated DMRs contain less CpGs than maternally methylated DMRs, Cytogenet. Genome Res. 113 (2006) 130–137.

[13] D. Jia, R.Z. Jurkowska, X. Zhang, A. Jeltsch, X. Cheng, Structure of Dnmt3a bound to Dnmt3L suggests a model for de novo DNA methylation, Nature 449 (2007) 248–251.

[14] Y. Hayashizaki, et al., Identification of an imprinted U2af binding protein related sequence on mouse chromosome 11 using the RLGS method, Nat. Genet. 6 (1994) 33–40.

[15] C. Plass, et al., Identification of Grf1 on mouse chromosome 9 as an imprinted gene by RLGS-M, Nat. Genet. 14 (1996) 106–109.

[16] T. Kaneko-Ishino, et al., Peg1/Mest imprinted gene on chromosome 6 identified by cDNA subtraction hybridization, Nat. Genet. 11 (1995) 52–59.

[17] Y. Kuroiwa, et al., Peg3 imprinted gene on proximal chromosome 7 encodes for a zinc finger protein, Nat. Genet. 12 (1996) 186–190.

[18] N. Miyoshi, et al., Identification of the Meg1/Grb10 imprinted gene on mouse proximal chromosome 11, a candidate for the Silver-Russell syndrome gene, Proc. Natl. Acad. Sci. U. S. A. 95 (1998) 1102–1107.

[19] N. Miyoshi, et al., Identification of an imprinted gene, Meg3/Gtl2 and its human homologue MEG3, first mapped on mouse distal chromosome 12 and human chromosome 14q, Genes Cells 5 (2000) 211–220.

[20] Y. Hagiwara, et al., Screening for imprinted genes by allelic message display: Identification of a paternally expressed gene impact on mouse chromosome 18, Proc. Natl. Acad. Sci. U. S. A. 94 (1997) 9249–9254.

[21] S. Kobayashi, et al., Mouse Peg9/Dlk1 and human PEG9/DLK1 are paternally expressed imprinted genes closely located to the maternally expressed imprinted genes: mouse Meg3/Gtl2 and human MEG3, Genes Cells 5 (2000) 1029–1037.

[22] Y. Mizuno, et al., Asb4, Ata3, and Dcn are novel imprinted genes identified by high-throughput screening using RIKEN cDNA microarray, Biochem. Biophys. Res. Commun. 290 (2002) 1499–1505.

[23] R. Schulz, et al., Chromosome-wide identification of novel imprinted genes using microarrays and uniparental disomies, Nucleic. Acids Res. 34 (2006) e88.

[24] A.J. Wood, et al., A screen for retrotransposed imprinted genes reveals an association between X chromosome homology and maternal germ-line methylation, PLoS Genet. 3 (2007) e20.

[25] P.P. Luedi, A.J. Hartemink, R.L. Jirtle, Genome-wide prediction of imprinted murine genes, Genome Res. 15 (2005) 875–884.

[26] M. Frommer, et al., A genomic sequencing protocol that yields a positive display of 5-methylcytosine residues in individual DNA strands, Proc. Natl. Acad. Sci. U. S. A. 89 (1992) 1827–1831.

[27] A.C. Ferguson-Smith, H. Sasaki, B.M. Cattanach, M.A. Surani, Parental-origin-specific epigenetic modification of the mouse H19 gene, Nature 362 (1993) 751–755.

[28] H. Shibata, et al., A methylation imprint mark in the mouse imprinted gene Grf1/Cdc25Mm locus shares a common feature with the U2afbp-rs gene: an association with a short tandem repeat and a hypermethylated region, Genomics 49 (1998) 30–37.

[29] S. Takada, et al., Epigenetic analysis of the Dlk1-Gtl2 imprinted domain on mouse chromosome 12: implications for imprinting control from comparison with Igf2-H19, Hum. Mol. Genet. 11 (2002) 77–86.

[30] V.M. Kalscheuer, E.C. Mariman, M.T. Schepens, H. Rehder, H.H. Ropers, The insulin-like growth factor type-2 receptor gene is imprinted in the mouse but not in humans, Nat. Genet. 5 (1993) 74–78.

[31] K. Okamura, et al., Comparative genome analysis of the mouse imprinted gene impact and its nonimprinted human homolog IMPACT: toward the structural basis for species-specific imprinting, Genome Res. 10 (2000) 1878–1889.

[32] U. Spiekerkoetter, et al., Uniparental disomy of chromosome 2 resulting in lethal trifunctional protein deficiency due to homozygous alpha-subunit mutations, Hum. Mutat. 20 (2002) 447–451.

[33] D.A. Thompson, et al., Retinal dystrophy due to paternal isodisomy for chromosome 1 or chromosome 2, with homoallelism for mutations in RPE65 or MERTK, respectively, Am. J. Hum. Genet. 70 (2002) 224–229.

[34] B. Chavez, E. Valdez, F. Vilchis, Uniparental disomy in steroid 5alpha-reductase 2 deficiency, J. Clin. Endocrinol. Metab. 85 (2000) 3147–3150.

[35] F.M. Petit, et al., Paternal isodisomy for chromosome 2 as the cause of Crigler–Najjar type I syndrome, Eur. J. Hum. Genet. 13 (2005) 278–282.

[36] R.J. Smith, W. Dean, G. Konfortova, G. Kelsey, Identification of novel imprinted genes in a genome-wide screen for maternal methylation, Genome Res. 13 (2003) 558–569.

[37] G. Piras, et al., Zac1 (Lot1), a potential tumor suppressor gene, and the gene for epsilon-sarcoglycan are maternally imprinted genes: identification by a subtractive screen of novel uniparental fibroblast lines, Mol. Cell. Biol. 20 (2000) 3308–3315.

[38] M.P. Lee, et al., Loss of imprinting of a paternally expressed transcript, with antisense orientation to KVLQT1, occurs frequently in Beckwith–Wiedemann syndrome and is independent of insulin-like growth factor II imprinting, Proc. Natl. Acad. Sci. U. S. A. 96 (1999) 5203–5208.

[39] J. Peters, et al., A cluster of oppositely imprinted transcripts at the Gnas locus in the distal imprinting region of mouse chromosome 2, Proc. Natl. Acad. Sci. U. S. A. 96 (1999) 3830–3835.

[40] N. Ruf, et al., Expression profiling of uniparental mouse embryos is inefficient in identifying novel imprinted genes, Genomics 87 (2006) 509–519.

[41] R. Kikuno, et al., HUGE: a database for human KIAA proteins, a 2004 update integrating HUGEppi and ROUGE, Nucleic. Acids Res. 32 (2004) D502–D504.

[42] F. Guillemot, A. Nagy, A. Auerbach, J. Rossant, A.L. Joyner, Essential role of Mash-2 in extraembryonic development, Nature 371 (1994) 333–336.

[43] T. Kono, et al., Birth of parthenogenetic mice that can develop to adulthood, Nature 428 (2004) 860–864.

[44] M. Kawahara, et al., High-frequency generation of viable mice from engineered bimaternal embryos, Nat. Biotechnol. 25 (2007) 1045–1050.

[45] T.L. Davis, J.M. Trasler, S.B. Moss, G.J. Yang, M.S. Bartolomei, Acquisition of the H19 methylation imprint occurs differentially on the parental alleles during spermatogenesis, Genomics 58 (1999) 18–28.

[46] T. Ueda, et al., The paternal methylation imprint of the mouse H19 locus is acquired in the gonocyte stage during foetal testis development, Genes Cells 5 (2000) 649–659.

[47] J.Y. Li, D.J. Lees-Murdock, G.L. Xu, C.P. Walsh, Timing of establishment of paternal methylation imprints in the mouse, Genomics 84 (2004) 952–960.

[48] H. Hiura, et al., DNA methylation imprints on the IG-DMR of the Dlk1–Gtl2 domain in mouse male germline, FEBS Lett. 581 (2007) 1255–1260.

[49] Y. Kato, et al., Role of the Dnmt3 family in de novo methylation of imprinted and repetitive sequences during male germ cell development in the mouse, Hum. Mol. Genet. 16 (2007) 2272–2280.

[50] B.J. Yoon, et al., Regulation of DNA methylation of Rasgrf1, Nat. Genet. 30 (2002) 92–96.

[51] A. Lewis, K. Mitsuya, M. Constancia, W. Reik, Tandem repeat hypothesis in imprinting: deletion of a conserved direct repeat element upstream of H19 has no effect on imprinting in the Igf2-H19 region, Mol. Cell. Biol. 24 (2004) 5650–5656.

[52] Y. Obata, et al., Post-implantation development of mouse androgenetic embryos produced by in-vitro fertilization of enucleated oocytes, Hum. Reprod. 15 (2000) 874–880.

[53] T. Koide, et al., A new inbred strain JF1 established from Japanese fancy mouse carrying the classic piebald allele, Mamm. Genome 9 (1998) 15–19.

[54] J.R. Nelson, et al., TempliPhi, phi29 DNA polymerase based rolling circle amplification of templates for DNA sequencing, Biotechniques Suppl. (2002) 44–47.

ORIGINAL ARTICLE

Endocrine Care

Cytochrome P450 Oxidoreductase Deficiency: Identification and Characterization of Biallelic Mutations and Genotype-Phenotype Correlations in 35 Japanese Patients

Maki Fukami, Gen Nishimura, Keiko Homma, Toshiro Nagai, Keiichi Hanaki, Ayumi Uematsu, Tomohiro Ishii, Chikahiko Numakura, Hirotake Sawada, Mariko Nakacho, Takanori Kowase, Katsuaki Motomura, Hidenori Haruna, Mihoko Nakamura, Akira Ohishi, Masanori Adachi, Toshihiro Tajima, Yukihiro Hasegawa, Tomonobu Hasegawa, Reiko Horikawa, Kenji Fujieda, and Tsutomu Ogata*

Context: Cytochrome P450 oxidoreductase (POR) deficiency is a rare autosomal recessive disorder characterized by skeletal dysplasia, adrenal dysfunction, disorders of sex development (DSD), and maternal virilization during pregnancy. Although multiple studies have been performed for this condition, several matters remain to be clarified, including the presence of manifesting heterozygosity and the underlying factors for clinical variability.

Objective: The objective of the study was to examine such unresolved matters by detailed molecular studies and genotype-phenotype correlations.

Patients: Thirty-five Japanese patients with POR deficiency participated in the study.

Results: Mutation analysis revealed homozygosity for R457H in cases 1–14 (group A), compound heterozygosity for R457H and one apparently null mutation in cases 15–28 (group B), and other combinations of mutations in cases 29–35 (group C). In particular, FISH and RT-PCR sequencing analyses revealed an intragenic microdeletion in one apparent R457H homozygote, transcription failure of apparently normal alleles in three R457H heterozygotes, and nonsense mediated mRNA decay in two frameshift mutation-positive cases examined. Genotype-phenotype correlations indicated that skeletal features were definitely more severe, and adrenal dysfunction, 46,XY DSD, and pubertal failure were somewhat more severe in group B than group A, whereas 46,XX DSD and maternal virilization during pregnancy were similar between two groups. Notable findings also included the contrast between infrequent occurrence of 46,XY DSD and invariable occurrence of 46,XX DSD and pubertal growth pattern in group A mimicking that of aromatase deficiency.

Conclusions: The results argue against the heterozygote manifestation and suggest that the residual POR activity reflected by the R457H dosage constitutes the underlying factor for clinical variability in some features but not other features, probably due to the simplicity and complexity of POR-dependent metabolic pathways relevant to each phenotype. (*J Clin Endocrinol Metab* 94: 1723–1731, 2009)

Cytochrome P450 oxidoreductase (POR) deficiency (PORD) is a rare autosomal recessive disorder caused by mutations in the gene encoding an electron donor for all microsomal P450 enzymes and several non-P450 enzymes (1–4). Salient clinical features of PORD include skeletal dysplasia

referred to as Antley-Bixler syndrome (ABS), adrenal dysfunction, 46,XY and 46,XX disorders of sex development (DSD), and maternal virilization during pregnancy (3, 4). Such features are primarily ascribed to impaired activities of POR-dependent CYP51A1 (lanosterol 14α-demethylase) and SQLE

Abbreviations: ABS, Antley-Bixler syndrome; CHX, cycloheximide; DSD, disorders of sex development; E₂, estradiol; FISH, fluorescent *in situ* hybridization; hCG, human chorionic gonadotropin; M, metabolite; NMD, nonsense-mediated mRNA decay; PCO, polycystic ovary; POR, cytochrome P450 oxidoreductase; PORD, POR deficiency; 17-OHP, 17α-hydroxyprogesterone; T, testosterone.

<zjs;> • <zjss;1,11>
<zshorttitle>Cytochrome P450 Oxidoreductase Deficiency: Genotype-Phenotype Correlations in Japanese